

AD-A198 364

## DOCUMENTATION PAGE

1a. REPORT SECURITY

1b. RESTRICTIVE MARKINGS

DTIC FILE COPY

2a. SECURITY CLASSIFICATION AUTHORITY

3. DISTRIBUTION / AVAILABILITY OF REPORT

2b. DECLASSIFICATION / DOWNGRADING SCHEDULE  
Unclassified

Approved for public release; distribution unlimited.

4. PERFORMING ORGANIZATION REPORT NUMBER(S)

5. MONITORING ORGANIZATION REPORT NUMBER(S)

N00014-79-C-0647

6a. NAME OF PERFORMING ORGANIZATION

6b. OFFICE SYMBOL  
(if applicable)

7a. NAME OF MONITORING ORGANIZATION

Colorado State University

6c. ADDRESS (City, State, and ZIP Code)

7b. ADDRESS (City, State, and ZIP Code)

Department of Chemistry  
Fort Collins, Colorado 30523

8a. NAME OF FUNDING / SPONSORING ORGANIZATION

8b. OFFICE SYMBOL  
(if applicable)

9. PROCUREMENT INSTRUMENT IDENTIFICATION NUMBER

Office of Naval Research

N00014-79-C-0647

8c. ADDRESS (City, State, and ZIP Code)

10. SOURCE OF FUNDING NUMBERS

800 North Quincy Street  
Arlington, VA 22217PROGRAM  
ELEMENT NO.PROJECT  
NO.TASK  
NO.WORK UNIT  
ACCESSION NO

11. TITLE (Include Security Classification)

"Benzene Clustered with N<sub>2</sub>, CO<sub>2</sub>, and CO: Energy Levels, Vibrational Structure and Nucleation"

12. PERSONAL AUTHOR(S)

R. Nowak, J.A. Menapace, E.R. Bernstein

13a. TYPE OF REPORT

13b. TIME COVERED

14. DATE OF REPORT (Year, Month, Day)

15. PAGE COUNT

Technical Report

FROM TO

July 12, 1988

16. SUPPLEMENTARY NOTATION The view, opinions, and/or findings contained in this report are those of the author(s) and should not be construed as an official Department of the Army position, policy, or decision, unless so designated by other documentation.

17. COSATI CODES

18. SUBJECT TERMS (Continue on reverse if necessary and identify by block number)

FIELD GROUP SUB-GROUP

clusters, van der Waals modes, supersonic jet spectroscopy, nucleation, benzene. (JES) ←

19. ABSTRACT (Continue on reverse if necessary and identify by block number)

See Attached

DTIC  
CTE  
AUG 15 1988  
S E D

20. DISTRIBUTION / AVAILABILITY OF ABSTRACT

☒ UNCLASSIFIED/UNLIMITED ☐ SAME AS RPT. ☐ DTIC USERS

21. ABSTRACT SECURITY CLASSIFICATION

UNCLASSIFIED

22a. NAME OF RESPONSIBLE INDIVIDUAL

22b. TELEPHONE (Include Area Code)

22c. OFFICE SYMBOL

Elliot R. Bernstein

303-491-6347

## **DISCLAIMER NOTICE**

**THIS DOCUMENT IS BEST QUALITY  
PRACTICABLE. THE COPY FURNISHED  
TO DTIC CONTAINED A SIGNIFICANT  
NUMBER OF PAGES WHICH DO NOT  
REPRODUCE LEGIBLY.**

OFFICE OF NAVAL RESEARCH

REPORT NUMBER N00014-72-C-0047

TECHNICAL REPORT #11

"REACTIVE COLLISIONS WITH  $N_2$ ,  $CO_2$  AND  $CO$   
ENERGY LEVELS, VIBRATIONAL STRUCTURE AND NUCLEATION"

by

R. Nowak, J. A. Mosper, and R. Bernstein

Prepared for Publication  
in the  
Journal of Chemical Physics

Department of Chemistry  
Colorado State University  
Fort Collins, Colorado 80523

July 1988

Reproduction in whole or in part is permitted for  
any purpose of the United States Government.

This document has been approved for public release  
and sale; its distribution is unlimited.

Accession For	
NTIS GRA&I	<input checked="" type="checkbox"/>
DTIC TAB	<input type="checkbox"/>
Unannounced	<input type="checkbox"/>
Justification	
By	
Distribution/	
Availability Codes	
Dist	Avail and/or Special
A-1	23 JR



**Benzene Clustered with  $N_2$ ,  $CO_2$ , and  $CO$ : Energy Levels,  
Vibrational Structure and Nucleation<sup>+</sup>**

by

R. Nowak, J.A. Menapace<sup>a)</sup> and E.R. Bernstein

Condensed Matter Sciences Laboratory  
Department of Chemistry  
Colorado State University  
Fort Collins, Colorado 80523

a) Present address: Frank J. Seiler Research Laboratory, U.S. Air  
Force Academy, Colorado Springs, Colorado 80848

<sup>+</sup>Supported in part by Philip Morris U.S.A. and ONR.

## ABSTRACT

Two color time of flight mass spectroscopy is employed to study the van der Waals (vdW) clusters of benzene( $N_2$ ) $_n^+$  ( $n \leq 8$ ), benzene( $CO_2$ ) $_n^+$  ( $n \leq 7$ ), and benzene( $CO$ ) $_n^+$  ( $n=1,2$ ) created in a supersonic molecular jet. Potential energy calculations of cluster geometries, normal coordinate analysis of vdW vibrational modes, and calculations of the internal rotational transitions are employed for the assignment of the benzene(solvent) $_1^+$  cluster spectra in the  $0_0^0$  and  $6_0^1$  regions of the benzene  $^1B_{2u} \rightarrow ^1A_{1g}$  transition. The respective vibronic and rotational selection rules for these clusters are determined based on the appropriate point groups and molecular symmetry groups of the clusters. Good agreement between the calculated and experimental spectra is obtained with regard to the vdW vibrational and internal rotational modes. The solvent molecules rotate nearly freely with respect to benzene about the benzene-solvent bond axis in the benzene(solvent) $_1^+$  clusters. In the excited state a small ca.  $20 \text{ cm}^{-1}$  barrier to rotation is encountered. Studies of larger clusters ( $n > 2$ ) reveal a broad red shifted single origin in the  $6_0^1$  spectra. A linearly increasing cluster energy shift is observed as a function of cluster size. The cluster energy shifts are not saturated by one solvent molecule on each side of the aromatic ring; several solvent molecules effectively interact with the solute  $\pi$  electronic cloud. Both homogeneous and inhomogeneous nucleation take place for the clusters studied depending on the ratio of the solvent-solvent binding energy to the cluster binding energy.

page 1

## I. INTRODUCTION.

Supersonic molecular jet spectroscopy has made possible studies of a wide variety of weakly bound molecular van der Waals (vdW) clusters. vdW clusters only slightly perturb the properties of their individual constituents and are characterized by relatively low binding energies, large intermolecular equilibrium distances, and low frequency intermolecular vibrational vdW modes.

A number of cluster systems, including, for example, vdW complexes of aromatic molecules (e.g., benzene and toluene) with hydrocarbon solvents,<sup>1,2</sup> and clusters of N-heterocyclic solutes (e.g., pyrazine and pyrimidine) with both alkane<sup>3,4</sup> and hydrogen bonding solvents (e.g., water and ammonia),<sup>4</sup> have been studied in our laboratory. Cluster geometries, energetics and energy dynamics have been explored in these systems yielding insight into nucleation processes and solvation geometries in both gas and condensed phase systems.

Our recent studies of the vdW cluster torsional mode structure in benzene-methane,<sup>5</sup> -deuteromethane, and -carbon tetrafluoride<sup>6</sup> clusters reveal that these clusters are rigid with regard to internal rotation of the cluster constituents. The internal torsional motion is found to be oscillatory and constrained by an orientationally dependent intermolecular potential with a barrier height of the order of the cluster binding energy. Given the geometries of the systems studied, the rigidity of the clusters can be understood by considering the nature of the solvent rotational dynamics; a low barrier one-dimensional rotation of the solvent molecule around the three-fold solute-solvent bond axis is not possible due to the orientation of the solvent molecule rotational axes.

In this paper we report spectroscopic results for the benzene(N<sub>2</sub>)<sub>1</sub>, benzene(CO)<sub>1</sub>, and benzene(CO<sub>2</sub>)<sub>1</sub> clusters: these systems exhibit almost free one-dimensional internal rotation between the cluster solute and solvent.

Benzene is chosen as a chromophore molecule since the formation of small clusters with benzene is relatively well understood. The high symmetry of benzene makes the interpretation of cluster geometries and theoretical calculations of rotational and vibrational modes relatively straightforward. The experimental spectroscopic results (two color time of flight mass spectroscopy (TOFMS)) are interpreted with the aid of calculational modeling of selected cluster characteristics, such as geometries, binding energies, and vdW vibrational and rotational energy level structures. Cluster geometry and favorable orientation of the solvent rotational axis permit one-dimensional internal rotational motion for these clusters. The analysis of the internal rotational energy levels of the vdW clusters studied bears some resemblance to that carried out for substituent groups in non-rigid aromatic molecules such as toluenes<sup>7</sup> and xylenes.<sup>8</sup>

The second part of this paper is devoted to spectroscopic studies of relatively large benzene(N<sub>2</sub>)<sub>n</sub> (n≤8), benzene(CO)<sub>n</sub> (n=1,2) and benzene(CO<sub>2</sub>)<sub>n</sub> (n≤7) clusters. Studies of the formation (nucleation) of large clusters are important since these clusters are potential model systems for condensed phases and because of an intense interest in nucleation and growth of aerosol particles. We have previously determined<sup>1,2</sup> that small (n=1,2) vdW clusters of benzene and toluene with hydrocarbon solvents (methane, ethane, propane) are formed via solute collisions with solvent dimers, trimers, and larger aggregates. Both homogeneous and inhomogeneous nucleation take place for these systems depending on the cluster binding energy compared to the solvent-solvent binding energy.

Larger vdW clusters with n>3 have not previously been extensively studied spectroscopically due to the difficulties in obtaining their resolved optical spectra. Consequently, little spectroscopic information concerning

these clusters is available. On the other hand, other techniques, such as e.g. electron diffraction<sup>9,10</sup> and infrared spectroscopy<sup>11</sup> are typically used for studies of much larger aggregates ( $n > 10^2$ ) but do not give specific information about the cluster energetics and geometries.

## II. EXPERIMENTAL PROCEDURES.

### A. Spectroscopic Techniques.

The  $S_1 \leftarrow S_0$  absorption spectra of the clusters are obtained using a pulsed supersonic molecular jet expansion and two color TOFMS. The details of the experimental apparatus and techniques employed have been described earlier.<sup>1,2</sup> Two synchronized Nd<sup>3+</sup>/YAG pumped dye lasers are used to probe both the origin and the  $6_0^1$  regions of the benzene  ${}^1B_{2u} \leftarrow {}^1A_{1g}$  transition in the cluster. Exciton LDS 698 dye is used for the pump laser with the output frequency doubled and mixed with the 1.064  $\mu\text{m}$  fundamental of the Nd<sup>3+</sup>/YAG laser. Either Exciton LDS 698 (doubled and mixed) or F 548 (doubled) dyes are used for the ionization laser. The energy of the ionization laser is typically lowered to the ionization threshold to limit cluster fragmentation upon ionization. The spectra are recorded using a boxcar averager, transient digitizer and computer.

Typically, 3-5% mixtures of the solvent gases with helium as a carrier gas are passed through a liquid benzene trap at room temperature and subsequently expanded into the apparatus vacuum chamber by using a pulsed nozzle. A nozzle backing pressure of 100 psi is typically used and the chamber pressure is maintained below  $4 \times 10^{-6}$  torr.

### B. Calculations of Cluster Geometries.

The cluster ground state geometries and binding energies are calculated for small clusters ( $n=1,2$ ) via an intermolecular potential energy minimization procedure employing the methods previously described.<sup>1,2</sup> A



Lennard-Jones (L-J; 6-12-1) potential is used with the atom-atom interaction parameters previously reported for similar calculations. The potential form and calculational algorithm yield consistent results with regard to the number of cluster configurations observed experimentally, their respective binding energies, and qualitative geometries (symmetries).

### III. THEORETICAL ANALYSIS OF CLUSTER VIBRATIONAL AND INTERNAL ROTATIONAL MOTION.

#### A. Normal Coordinate Analysis of vdW Vibrations and Vibronic Transitions.

The normal coordinate analysis (NCA) of the cluster vdW vibrations is performed by using the same methods as described in our previous publication<sup>5</sup> on vdW cluster vibronic structure. The GF method of Wilson<sup>13</sup> is employed in which the cluster constituent force fields are generated by using the central force approximation including out-of-plane motion terms. The intramolecular force constants chosen correspond to general functional group stretches and bends.<sup>14</sup> The intermolecular force constants are generated as second derivatives of the intermolecular L-J potential discussed above. The GF matrix is numerically diagonalized and the  $3N-6$  ( $3N-5$  in the present instance) nonzero eigenvector normal modes and eigenvalue energies are determined in the usual fashion. The reader is referred to our previous publication<sup>5</sup> for details of the theoretical procedures employed.

The eigenvector normal modes found based on the calculated geometries of the rigid clusters (point groups  $C_{2v}$  and  $C_s$ ) are 1. the vdW stretch ( $S_z$ ) which entails the motion of the solvent molecule in the direction perpendicular to the benzene molecular plane, 2. the vdW bends ( $b_x$  and  $b_y$ ) with translational motions parallel to the benzene ring (x or y directions), and 3. the vdW torsions ( $t_y$  and  $t_z$ ) which transform as the rotations of the cluster constituents about the y and z axes, respectively. These normal modes are

shown in Fig. 1 for the case of the rigid benzene(N<sub>2</sub>)<sub>1</sub> cluster. The t<sub>z</sub> torsional motion will not be present if the solvent molecule can undergo nearly free rotation about the cluster z axis, perpendicular to its bond axis. Instead, additional rotational levels will be present in the eigenstates. Of course, the C<sub>2v</sub> rigid cluster point group is no longer applicable for the description of the rotational levels and an appropriate molecular symmetry group must be used. We assume that all the low-lying intermolecular eigenstates other than t<sub>z</sub> are nearly harmonic.

The appropriate selection rules for vibronic transitions in the rigid cluster are determined by analyzing qualitatively transition moment matrix elements using the adiabatic approximation. In the C<sub>2v</sub> symmetry of the benzene(N<sub>2</sub>)<sub>1</sub> and benzene(CO<sub>2</sub>)<sub>1</sub> rigid clusters, the vdW vibronic transition selection rules for the 0<sub>0</sub><sup>0</sup> region in the absence of the Herzberg-Teller (HT) coupling are as follows:  $\Delta v = 0, \pm 1, \pm 2, \dots$  for the totally symmetric vdW stretch and  $\Delta v = 0, \pm 2, \pm 4, \dots$  for the nontotally symmetric vdW bends and torsions. In the 6<sub>0</sub><sup>1</sup> region the fundamental of the nontotally symmetric torsion (t<sub>z</sub>) is additionally allowed. This torsion is vibronically induced in the 0<sub>0</sub><sup>0</sup> region if HT coupling is active. For the C<sub>s</sub> symmetry of the benzene(CO)<sub>1</sub> rigid cluster, the vibronic selection rules for the 0<sub>0</sub><sup>0</sup> region are slightly different:  $\Delta v = 0, \pm 1, \pm 2, \dots$  for the vdW stretch S<sub>z</sub>, bend b<sub>x</sub>, and torsion t<sub>y</sub>, and  $\Delta v = 0, \pm 2, \pm 4, \dots$  for the bend b<sub>y</sub> and torsion t<sub>z</sub>. In C<sub>s</sub> symmetry all the vdW modes are capable of vibronic coupling and, hence,  $\Delta v = 0, \pm 1, \pm 2, \dots$  if HT coupling is present.  $\Delta v = 0, \pm 1, \pm 2, \dots$  for all the vdW modes even in the absence of HT coupling for this latter cluster in the 6<sub>0</sub><sup>1</sup> region.

#### B. Internal Rotational Analysis of the t<sub>z</sub> Torsional Mode.

We assume in the present analysis that the solvent molecule can rotate in one-dimension about its axis of largest moment of inertia, i.e., the

axis perpendicular to the N-N (C=O) molecular bond and passing through the solvent and solute molecular center of mass. The rotational axes for N<sub>2</sub> and CO<sub>2</sub> in the cluster correspond to the solute-solvent bond (cluster z) axis (benzene six-fold symmetry axis) and the CO rotational axis is found to form a ca. 15° angle with the benzene six-fold axis. The appropriate molecular symmetry group<sup>15</sup> must be used in the determination of the rotational mode structure and selection rules.

Analysis of the internal rotational transitions in these clusters is performed by using the same approach as described in our previous publication<sup>8</sup> for internal rotations in non-rigid aromatic molecules. The energy levels and wavefunctions for the motion of a one-dimensional hindered rotor are obtained by solving the Schrödinger equation

$$\left[ -B \frac{\partial^2}{\partial \phi^2} + V(\phi) \right] \psi_m(\phi) = E_m \psi_m(\phi), \quad (1)$$

in which the potential form for the benzene clusters considered is approximated by

$$V(\phi) = \frac{1}{2} V_6 (1 - \cos 6\phi). \quad (2)$$

In eq. (1) B is the rotational constant ( $h^2/8\pi^2 cI$ ), I is the moment of inertia, and  $\phi$  is the torsional angle for the N<sub>2</sub>, CO<sub>2</sub> and CO rotors. The solution of the Schrödinger equation for a free rotor ( $V(\phi)=0$ ) is of the form

$$\psi_m(\phi) = \frac{1}{\sqrt{2\pi}} e^{\pm im\phi} \quad (3)$$

and the free rotor energy levels are

$$E_m = m^2 B. \quad (4)$$

The eigenvalues and eigenvectors of the hindered rigid rotor Hamiltonian eq. (1) are solved for within a basis set of 21 free rotor eigenfunctions. The

parameter  $V_6$  is adjusted to fit the energy levels of the hindered rotor to the experimental data.

The energy levels for rotation of the solvent with respect to the solute are labeled according to the  $m$  quantum numbers of a one-dimensional rotor. The symmetry of the Hamiltonian is given by the appropriate molecular symmetry group:<sup>15</sup>  $G_{24}^5$  for the benzene(N<sub>2</sub>)<sub>1</sub> and benzene(CO<sub>2</sub>)<sub>1</sub> clusters, and  $G_{12}^3$  for the benzene(CO)<sub>1</sub> cluster (according to the notation in ref. 16). The symmetry allowed rotational transitions within the  $0_0^0$  and  $6_0^1$  bands are determined via the nonvanishing integral rule taking into account the correlation between the molecular symmetry group of benzene and the appropriate molecular symmetry groups of the clusters. The results of this analysis for different clusters are given in Table I. The  $a_{1g} \leftrightarrow a_{1g}$  ( $a_1 \leftrightarrow a_1$ ) and  $b_{2u} \leftrightarrow b_{2u}$  ( $b_2 \leftrightarrow b_2$ ) transitions are not allowed at the origin but are allowed at  $6_0^1$ . The  $e_{2g} \leftrightarrow e_{2g}$  ( $e_2 \leftrightarrow e_2$ ),  $e_{1u} \leftrightarrow e_{1u}$  ( $e_1 \leftrightarrow e_1$ ),  $a_{1g} \leftrightarrow e_{2g}$  ( $a_1 \leftrightarrow e_2$ ) and  $e_{1u} \leftrightarrow b_{2u}$  ( $e_1 \leftrightarrow b_2$ ) transitions are allowed in both spectral regions. This finding is important for the interpretation and assignments of the spectra, particularly in the  $0_0^0$  region. The dependence of the energy of each internal rotational level on the parameter  $V_6$  is illustrated for the case of the benzene(N<sub>2</sub>)<sub>1</sub> cluster in Fig. 2. Similar dependences are obtained for the benzene(CO)<sub>1</sub> and benzene(CO<sub>2</sub>)<sub>1</sub> clusters. In the latter case the spacings between individual rotational levels are relatively smaller due to a larger moment of inertia of the CO<sub>2</sub>.

Some of the allowed transitions may not be observed due to nuclear spin selection rules. Moreover, the different nuclear spin states associated with various rotational levels result in hot bands which cannot be removed from the spectra by normal cooling techniques. For the benzene(N<sub>2</sub>)<sub>1</sub> and benzene(CO<sub>2</sub>)<sub>1</sub> clusters ( $G_{24}^5$  molecular symmetry group) only the "g" internal rotational

levels are populated with the following relative statistical weights:  $a_{1g} : e_{1u} : b_{2u} : e_{2g} = 1 : 0 : 0 : 2$ . "g" and "u" type levels are not distinguished in the  $G_{12}^3$  molecular symmetry group and all the different rotational symmetry levels of benzene(CO)<sub>1</sub> may be populated. The relative statistical weights are, in this latter case,  $a_1 : e_1 : b_2 : e_2 = 1 : 2 : 1 : 2$ .

#### IV. BENZENE (SOLVENT)<sub>1</sub> CLUSTERS SPECTRA, CALCULATIONS AND ASSIGNMENTS.

A similar approach to spectral analysis consisting of calculating the internal rotational and vibrational transitions is employed for all three benzene (solvent)<sub>1</sub> clusters studied. Therefore, only the assignments for the benzene(N<sub>2</sub>)<sub>1</sub> spectra are discussed in detail; other cluster spectra are analyzed based on the same arguments.

##### A. Benzene(N<sub>2</sub>)<sub>1</sub>.

The results of calculations of the ground state geometry and vdW vibrations of the benzene(N<sub>2</sub>)<sub>1</sub> cluster are shown in Fig. 1. The calculations yield a single cluster geometry with the solvent molecule located in the plane parallel to benzene at a distance 3.3 Å above the center of the benzene ring. The calculated ground state binding energy is  $-501 \text{ cm}^{-1}$ . No other local potential minima are found in the calculations. The eigenvectors of the vibrational vdW modes and their corresponding energies calculated from the NCA are shown in Fig. 1. Rotating the N<sub>2</sub> molecule by an angle  $30^\circ$  around the z axis (N<sub>2</sub> rotational axis) results in an increase of the calculated binding energy by only ca.  $1 \text{ cm}^{-1}$ . This indicates no barrier to rotation in the ground state and suggests that the N<sub>2</sub> molecule can rotate in the cluster with little barrier to rotation.

The spectra of the benzene(N<sub>2</sub>)<sub>1</sub> cluster in the  $0_0^0$  and  $6_0^1$  regions of the benzene  ${}^1B_{2u} \leftarrow {}^1A_{1g}$  transition are shown in Fig. 3. Such spectra are typi

cally understood<sup>5</sup> based on allowed origins for the  $0_0^0$  and  $6_0^1$  regions and a set of assigned vdW normal modes built on these origins. The origin in the cluster  $0_0^0$  spectrum (if allowed) would typically exhibit a shift in energy from the benzene  $0_0^0$  transition similar to that observed in the  $6_0^1$  spectrum of the cluster. For the benzene( $N_2$ )<sub>1</sub> cluster this shift equals  $-6\text{ cm}^{-1}$ . We are not able to understand these spectra and find appropriate assignments based on this now standard approach, however. The  $0_0^0$  spectrum, at least, must be analyzed in the light of the proper group theory and the vdW rotation-vibration energy level set discussed above.

If the  $N_2$  molecule in the benzene( $N_2$ )<sub>1</sub> cluster were freely rotating in both  $S_0$  and  $S_1$ ,  $0a_{1g} \leftarrow 0a_{1g}$ ,  $1e_{1u} \leftarrow 1e_{1u}$ ,  $2e_{2g} \leftarrow 2e_{2g}$ , and  $4e_{2g} \leftarrow 4e_{2g}$   $t_z$  rotational transitions (replacing the  $t_z$  vdW mode) would coincide in energy and give only one peak at the origin. The first two of these transitions are not allowed in the  $0_0^0$  region due either to vibronic or nuclear spin selection rules (see Table I). If the barrier to rotation changes upon  $S_1 \leftarrow S_0$  excitation, the energies of the  $2e_{2g} \leftarrow 2e_{2g}$  and  $4e_{2g} \leftarrow 4e_{2g}$  transitions would be different; if the magnitude of the change were small, a doublet would be produced in the spectrum. Thus an intense doublet in the spectrum most probably corresponds to the allowed  $2e_{2g} \leftarrow 2e_{2g}$  and  $4e_{2g} \leftarrow 4e_{2g}$  transitions.

A reasonable fit to the  $0_0^0$  spectrum is obtained by assuming that in the cluster ground state the  $N_2$  molecule can freely rotate around the benzene- $N_2$  bond and in the excited state the rotation is slightly hindered by a ca.  $20\text{ cm}^{-1}$  potential barrier. The final calculated spectrum shown in Fig. 3a is a superposition of both one-dimensional rotor and vdW vibrational transitions; due to the rotational degree of freedom, the  $t_z$  torsion is not taken into account in the vibrational analysis. Specific assignments of the calculated and experimental spectra are given in Table II. As can be seen in Fig. 3a and

Table II the agreement between the experimental and calculated spectrum is very good. The fit is considerably worsened if the rotational barrier in either state is changed more than  $10 \text{ cm}^{-1}$ .

The  $6_0^1$  spectrum is easier to analyze since in this case the origin transition is allowed (compare Table I). The strongest feature in the spectrum in Fig. 3b, shifted by  $-6 \text{ cm}^{-1}$  with respect to the benzene  $6_0^1$  transition, is unambiguously ascribed to the cluster  $6_0^1$  origin. A single origin is observed in agreement with the single calculated cluster geometry shown in Fig. 1. The spectral features observed to the red of the origin are assigned as hotbands since their intensity changes considerably with the carrier gas backing pressure but not with ionization energy. Several relatively weak peaks observed to the blue of the cluster  $6_0^1$  origin are vdW vibrational and rotational bands: their assignments are given in Table II. The  $6_0^1$  spectrum is more than an order of magnitude more intense than the  $0_0^0$  spectrum, with relatively intense vdW vibrations built on the allowed  $6_0^1$  origin. The rotational transitions which are seen in the  $0_0^0$  spectrum are almost entirely hidden under the  $6_0^1$  origin spectrum. Moreover, in the region ca.  $15 \text{ cm}^{-1}$  to the blue of the cluster origin (around the benzene  $6_0^1$  transition), where some of the rotational transitions are calculated to appear, the mass detector is still saturated by the ionized benzene molecule signal. This effect eliminates observation of any weak features and is visualized by a dip in the spectrum. Further to the blue only weak rotational transitions may be present along with vdW vibrations as indicated in the  $6_0^1$  spectrum in Fig. 3b.

Calculations of the rotational barrier, rotational energy levels, and vdW vibrations confirm that the benzene( $\text{N}_2$ )<sub>1</sub> cluster  $0_0^0$  spectrum must be assigned as a superposition of both one-dimensional rotor and vdW vibrational transitions. This approach gives the best and most satisfactory assignment of

the spectral features in agreement with the selection rules given in Table I. In order to reproduce more accurately the most intense features in the spectrum a small, ca.  $20\text{ cm}^{-1}$ , barrier to rotation in the excited electronic state is assumed.

The cluster energy shifts as compared to transitions in benzene are  $36\text{ cm}^{-1}$  and  $-6\text{ cm}^{-1}$  for the  $0_0^0$  and the  $6_0^1$  transitions, respectively. This unexpected difference in shifts must arise from local changes of polarizability upon excitation of the benzene and can only partially be explained by the change of the benzene  $6^1$  vibration in the cluster. At present we do not have a satisfactory explanation for these apparently different cluster shifts.

#### B. Benzene(CO<sub>2</sub>)<sub>1</sub>.

The  $0_0^0$  and  $6_0^1$  spectra of the benzene(CO<sub>2</sub>)<sub>1</sub> cluster are shown in Fig. 4. The cluster energy shifts are  $-1\text{ cm}^{-1}$  and  $4\text{ cm}^{-1}$ , for the  $0_0^0$  and  $6_0^1$  transitions, respectively. One cluster configuration, almost identical to the nitrogen case (shown in Fig. 1), is calculated for benzene(CO<sub>2</sub>)<sub>1</sub> with the binding energy  $-868\text{ cm}^{-1}$ .

The arguments given above for the assignment of benzene(N<sub>2</sub>)<sub>1</sub> cluster are valid in the present case, since both cluster symmetries and selection rules are identical. The specific assignments of both spectra in Fig. 4 are given in Table III. The CO<sub>2</sub> barrier for rotation in the excited state is taken to be  $16\text{ cm}^{-1}$  and good fit to the  $0_0^0$  experimental spectrum is obtained as shown in Fig. 4a. The relatively smaller energies of particular rotational transitions of the benzene(CO<sub>2</sub>)<sub>1</sub> cluster compared to the benzene(N<sub>2</sub>)<sub>1</sub> cluster arise because the moment of inertia for CO<sub>2</sub> ( $B = 1.547\text{ cm}^{-1}$ ) is larger than for N<sub>2</sub>.

The  $6_0^1$  spectrum in Fig. 4b shows a strong origin peak with several weak transitions to the blue. These weak transitions can again be assigned (Table



III) as internal rotations and vdW vibrations. The origin corresponds to a single calculated cluster geometry.

### C. Benzene(CO)<sub>1</sub>.

A single cluster geometry shown in Fig. 5 is calculated for the benzene(CO)<sub>1</sub> cluster with the binding energy -612 cm<sup>-1</sup>. The CO molecule is located 3.24 Å above the benzene ring forming a 15° angle with the benzene molecular plane in such a way that the oxygen lies closer to benzene than does the carbon atom. The rigid cluster symmetry is C<sub>s</sub> instead of the C<sub>2v</sub> symmetry found for N<sub>2</sub> and CO<sub>2</sub> clusters. The CO rotational axis is no longer parallel to the benzene six-fold axis, the axes forming a 15° angle with respect to one another. Therefore, if an internal rotation is present, the CO rotational axis must be undergoing a small precessional motion in order to avoid a high potential barrier to rotation. The appropriate selection rules for the rotational transitions are based on the G<sub>12</sub><sup>3</sup> molecular symmetry group (see Table I).

Assignment of the benzene(CO)<sub>1</sub> spectra is similar to the assignment of the benzene(N<sub>2</sub>)<sub>1</sub> spectra, except for the above mentioned selection rules. The calculated and experimental spectra are compared in Fig. 6, with their specific assignments given in Table IV. The benzene(CO)<sub>1</sub> spectra are similar to the analogous benzene(N<sub>2</sub>)<sub>1</sub> spectra since both these clusters are of identical masses, have very similar geometries, and N<sub>2</sub> and CO have almost identical rotational constants (B = 1.915 cm<sup>-1</sup> for CO and 1.917 cm<sup>-1</sup> for N<sub>2</sub>). Consequently, both clusters exhibit similar vdW vibrations and have similar energies for rotational transitions; however, fewer and broader bands are observed in the benzene(CO)<sub>1</sub> spectrum in Fig. 6a compared to the spectrum of benzene(N<sub>2</sub>)<sub>1</sub> in Fig. 3a, due to an increased number of allowed transitions for benzene(CO)<sub>1</sub> clusters (Table I). The overlap of transitions is also responsible for the

change of the relative intensities in the  $0_0^0$  benzene(CO)<sub>1</sub> spectrum as compared to the  $0_0^0$  spectra of the analogous clusters of N<sub>2</sub> and CO<sub>2</sub>.

The  $6_0^1$  spectrum in Fig. 6b is well assigned as a superposition of rotational and vdW vibrational mode transitions (Table IV). The spectrum is dominated by a strong origin and vdW vibrations, although weak rotational transitions can also be distinguished.

## V. BENZENE(SOLVENT)<sub>2</sub> CLUSTERS.

The analysis of the benzene(solvent)<sub>2</sub> cluster spectra differs from the detailed approach taken for the benzene(solvent)<sub>1</sub> cluster spectra presented above since the benzene(solvent)<sub>2</sub> spectra are less well resolved and thus do not contain sufficient experimental information about possible vibrations and/or rotations. The analysis of the benzene(solvent)<sub>2</sub> cluster spectra is based primarily on calculations of cluster geometries and assignment rules determined in our previous studies<sup>1-6</sup> of other vdW clusters.

### A. Benzene(N<sub>2</sub>)<sub>2</sub>.

Two ground state minimum energy cluster geometries are calculated for the benzene(N<sub>2</sub>)<sub>2</sub> cluster (Fig. 7). The isotropic configuration with binding energy of -1007 cm<sup>-1</sup> features a nitrogen molecule on either side of the aromatic ring. In the anisotropic geometry both nitrogen molecules are attached to one side of the benzene ring with the binding energy -962 cm<sup>-1</sup>. No other local minima are found in the potential energy calculations.

The benzene(N<sub>2</sub>)<sub>2</sub> cluster spectra are not detected in the  $0_0^0$  region. This symmetry induced transition (forbidden in benzene) is certainly very weak for the isotropic cluster geometry, since the six-fold symmetry of benzene may be preserved in the cluster in some averaged sense, especially considering the rotations of the N<sub>2</sub> molecules. Why the anisotropic cluster spectrum is not observed is difficult to say. The  $6_0^1$  spectra taken at two different ioniza-

tion energies are shown in Fig. 8. One relatively broad peak shifted  $-16\text{ cm}^{-1}$  to the red of benzene transition dominates both spectra. Another peak at  $-9\text{ cm}^{-1}$  visible as a shoulder on the main feature increases in intensity at lower ionization energies. This feature does not correspond to features in other mass channels. The two features, one at  $-16\text{ cm}^{-1}$  and the other at  $-9\text{ cm}^{-1}$ , are thus assigned to two different cluster geometries. The cluster whose  $6_0^1$  transition is at  $-16\text{ cm}^{-1}$  apparently has a higher ionization energy.

Benzene vdW clusters with other solvents<sup>1,2</sup> show that the energy shift for the isotropic cluster is larger than the energy shift for the analogous anisotropic cluster. This is due to a better overlap of the solvent molecules with the aromatic  $\pi$  cloud of benzene in the isotropic cluster, resulting in larger polarizability changes upon cluster excitation. Typically, the anisotropic benzene(solvent)<sub>2</sub> cluster exhibits a shift roughly equal to the one found for the benzene(solvent)<sub>1</sub> cluster. Given this assumption, the more shifted peak in the spectrum is assigned to the symmetrical (isotropic) cluster and the less shifted peak to the anisotropic cluster. Comparing the relative intensities of both features in the spectrum one concludes that the concentration of the benzene(N<sub>2</sub>)<sub>2</sub> isotropic cluster in the beam is greater than of the anisotropic cluster by roughly a factor of 2 or 3.

#### B. Benzene(CO<sub>2</sub>)<sub>2</sub>.

The benzene(CO<sub>2</sub>)<sub>2</sub> cluster spectra are detected in both the  $0_0^0$  and  $6_0^1$  regions and are shown in Fig. 9. The origin, shifted in both spectra  $-22\text{ cm}^{-1}$  to the red of the benzene transition (at  $0\text{ cm}^{-1}$ ), is ascribed to one cluster geometry. Clearly, another cluster geometry gives rise to a peak at  $-2\text{ cm}^{-1}$  in the  $0_0^0$  spectrum in Fig. 9a. This feature (geometry) is not seen in the  $6_0^1$  spectrum due to the saturation of the mass detector by ionized benzene precisely in this spectral region (see dip in the spectrum in Figure 9b). The

position of the second feature at  $-9\text{ cm}^{-1}$  in the  $6_0^1$  spectrum corresponds to the origin of the benzene(CO<sub>2</sub>)<sub>3</sub> cluster (compare with Figs. 11 and 12) and thus is ascribed to dissociation of this cluster giving rise to a signal in the benzene(CO<sub>2</sub>)<sub>2</sub> mass channel. Pronounced change of the relative intensity of this band with varying the ionization energy confirms this assignment.

In agreement with the experimental observation, two ground state minimum energy cluster geometries, similar to those found for benzene(N<sub>2</sub>)<sub>2</sub> cluster (shown in Fig. 7) are calculated. The binding energies are  $-1746\text{ cm}^{-1}$  and  $-1955\text{ cm}^{-1}$  for the isotropic and anisotropic clusters, respectively. The  $-22\text{ cm}^{-1}$  shifted origin in the two spectra is assigned to the isotropic cluster, whereas the  $2\text{ cm}^{-1}$  shifted origin in the  $0_0^0$  spectrum is assigned to the anisotropic cluster. As can be seen from the comparison of the relative intensities in Fig. 9a, the concentration of the isotropic cluster in the supersonic molecular jet is larger than the concentration of the anisotropic cluster. The intensity of the peak ascribed to the anisotropic cluster can be diminished by increasing the ionization energy. The behavior of the benzene(CO<sub>2</sub>)<sub>2</sub> cluster is thus very similar to the one reported above for the benzene(N<sub>2</sub>)<sub>2</sub> cluster.

### C. Benzene(CO)<sub>2</sub>.

Four cluster geometries (one isotropic and three anisotropic) are calculated for the benzene(CO)<sub>2</sub> cluster with the binding energies  $-1284\text{ cm}^{-1}$  and  $-1580\text{ cm}^{-1}$ ,  $-1601\text{ cm}^{-1}$  and  $-1697\text{ cm}^{-1}$ , respectively.

The  $6_0^1$  spectrum of the benzene(CO)<sub>2</sub> cluster (Fig. 10) is, different from the spectra of analogous clusters with N<sub>2</sub> and CO<sub>2</sub>. The spectrum is relatively weak and exhibits four distinct features at  $-56\text{ cm}^{-1}$ ,  $-61\text{ cm}^{-1}$ ,  $-75\text{ cm}^{-1}$  and  $-88\text{ cm}^{-1}$  with respect to the benzene origin. The strongest feature at  $-56\text{ cm}^{-1}$  probably corresponds to the isotropic calculated cluster geometry

which is found to occur with the largest probability.<sup>17</sup> The other features may be assigned to the other three calculated anisotropic cluster geometries.

The broad background in the spectrum is likely due to dissociation of higher order clusters but cannot be entirely eliminated by lowering the ionization energy. This may indicate that some of the peaks in the spectrum are due to dissociation of larger clusters instead of being inherently related to the benzene(CO)<sub>2</sub> clusters. Higher order clusters of benzene with CO are not, however, detected in these experiments.

#### VI. LARGE CLUSTERS - TRANSITION ENERGY SHIFTS.

Except for the benzene(CO<sub>2</sub>)<sub>3</sub> cluster spectrum shown in Fig. 11, spectra of large clusters are not detected in the 0<sub>0</sub><sup>0</sup> region. The benzene 0<sub>0</sub><sup>0</sup> transition is cluster symmetry induced and thus is not expected to be intense for low concentrations of specific clusters. One origin shifted by -9 cm<sup>-1</sup> is observed in the 0<sub>0</sub><sup>0</sup> spectrum of the benzene(CO<sub>2</sub>)<sub>3</sub> cluster.

The 6<sub>0</sub><sup>1</sup> spectra of benzene solvated by up to eight N<sub>2</sub> molecules and seven CO<sub>2</sub> molecules are shown in Figs. 12 and 13, respectively. Progressive transition energy shifts toward lower energies with increasing cluster size are observed for the large clusters. One rather broad peak dominates the spectra of N<sub>2</sub> clusters, whereas spectra of progressively larger CO<sub>2</sub> clusters are also generally broad but do show some structure on a broad background. The CO<sub>2</sub> cluster spectra are in addition somewhat obscured by a pronounced dip due to the saturation of the mass detector by ionized nonclustered benzene molecules. Plots of an average cluster transition energy shift as a function of cluster size are given in Fig. 14. A linear dependence of the energy shift on the cluster size is observed for n>2. Addition of each solvent molecule thus causes a similar perturbation of the benzene transition once the first two solvent molecules are attached. For clusters with seven and eight nitro-

gen molecules, the change in transition energy shift seems to be slightly smaller, possibly due to a gradually weaker interaction of the solvent molecules with the aromatic  $\pi$  cloud of benzene as the cluster size increases.

The above results suggest that the cluster shifts are not entirely saturated by one solvent molecule on each side of the aromatic ring, as is found for benzene-alkane<sup>1</sup> and toluene-alkane<sup>2</sup> clusters. Larger shifts still arise with addition of more than two molecules indicating that several solvent molecules may effectively interact with benzene. This is certainly the case for the solute-solvent systems studied here for which the sizes of linear solvent molecules are relatively small compared to benzene. The  $N_2$  clusters with benzene exhibit larger energy shifts than the corresponding clusters of  $CO_2$ , even though the  $CO_2$  molecule has a relatively larger polarizability. The increase of the energy shift with cluster size is also larger for benzene( $N_2$ )<sub>n</sub> than for benzene( $CO_2$ )<sub>n</sub>. This is probably due to the smaller size of the  $N_2$  molecule and thus a better spatial packing of nitrogen around the benzene and concomitant stronger interaction with the electric  $\pi$  cloud.

Many solvent molecules effectively interact with benzene and contribute to the cluster transition energy shift in large clusters. Since only one rather broad feature is observed in the large cluster spectra, the spectral energy differences between various cluster configurations must be relatively small. Comparison of the spectra of benzene( $N_2$ )<sub>n</sub> clusters with the spectra of benzene( $CO_2$ )<sub>n</sub> clusters suggests that the  $N_2$  clusters exhibit fewer and more unique orientations than the  $CO_2$  clusters; spectra of  $N_2$  clusters show one relatively narrow peak, while those of  $CO_2$  are broader and have some structure on the main background. This difference may be due to the larger size of the  $CO_2$  as compared to  $N_2$ . Calculations of the possible large cluster geometries are presently being carried out in order to confirm this interpretation.

Preliminary results indicate that clusters with more than two solvent molecules exhibit a large number of local potential energy minima differing slightly in cluster binding energy. The number of local minima increases with the cluster size.

If large clusters are to serve as potential models of condensed phase systems, gas to cluster energy shifts must be explored and compared with those of condensed phase solutions. The largest energy shift observed in our experiments for benzene( $N_2$ )<sub>n</sub> clusters is ca.  $-42\text{ cm}^{-1}$  for a cluster with eight  $N_2$  molecules. A shift of about  $-50\text{ cm}^{-1}$  is measured<sup>18</sup> for benzene dissolved in supercritical nitrogen fluid (in the gas phase) at a fluid density of ca.  $220\text{ kg m}^{-3}$  (at  $T = 295\text{ K}$  and  $P = \text{ca. } 300\text{ bar}$ ). This shift increases with increasing fluid density (pressure) due to forced crowding of the solvent around the solute so that more molecules effectively interact with benzene. In the liquid phase and high density fluid phase the energy shift increases up to  $-180\text{ cm}^{-1}$  due to the additional interaction of nitrogen molecules forced to crowd about the benzene molecule at its periphery.

Based on the comparison of benzene( $N_2$ )<sub>n</sub> cluster shifts with the supercritical nitrogen fluid results, one concludes that in the low density condensed phase "solvation" of benzene takes place mostly about the  $\pi$  system and not at the more repulsive C-H periphery positions. This latter type of solvation must be forced, however, in high density fluids and the liquid state.

## VII. NUCLEATION.

The nucleation process for small vdW clusters can be largely understood only if various spectral features can be ascribed to specific cluster geometries. Two basic types of nucleation can be distinguished: homogeneous nucleation in which solvent molecules are added to the solute molecule or cluster one molecular at a time; and inhomogeneous nucleation in which more

than one solvent molecule is added to the solute or cluster at a given time. Relative intensity data for clusters of benzene and toluene with hydrocarbon solvents has led to the conclusion that solvent molecules exist in the supersonic expansion in the form of dimers or larger aggregates and that isotropic benzene(solvent)<sub>2</sub> clusters are homogeneously nucleated and anisotropic clusters are inhomogeneously nucleated.<sup>1,2</sup> Whether homogeneous nucleation (isotropic clusters) or inhomogeneous nucleation (anisotropic clusters) arises depends on the relative size of the solvent dimer binding energy ( $E_d$ ) with respect to the solute-solvent (cluster) binding energy ( $E_c$ ) in the cluster. The smaller the binding energy of a solvent dimer compared to the binding energy of the cluster, the higher the concentration of isotropic clusters. Inhomogeneous nucleation is found to predominate for small clusters of benzene and toluene with two hydrocarbon solvent molecules because  $E_d/E_c$  is relatively large (0.3 - 0.8 depending on the solvent).

The binding energies of N<sub>2</sub> and CO<sub>2</sub> dimers are, however, quite small: -150 cm<sup>-1</sup> and -442 cm<sup>-1</sup>, respectively. As shown in Table V the  $E_d/E_c$  value for the benzene(N<sub>2</sub>)<sub>2</sub> and benzene(CO<sub>2</sub>)<sub>2</sub> clusters is only 0.15 and 0.23, respectively. This clearly favors homogeneous nucleation and formation of isotropic clusters, since solvent dimers can easily be dissociated with very little excess energy. Our spectra confirm this implication because in all cases studied the peak ascribed to isotropic benzene(solvent)<sub>2</sub> clusters is much more intense than the peak due to anisotropic clusters. This effect is especially strong in the case of N<sub>2</sub> clusters for which  $E_d/E_c$  is small.

Clusters larger than benzene(solvent)<sub>2</sub> are most likely formed by inhomogeneous nucleation. First, larger solvent clusters have larger binding energy. High solvent aggregate binding energy favors inhomogeneous nucleation. Comparison of the calculated solvent dimer and trimer binding energies



given in Table V shows an almost threefold increase of the solvent aggregate binding energy ( $E_a$ ) for the trimer with respect to the dimer. At the same time only a twofold increase of the cluster binding energy takes place for the benzene (solvent)<sub>2</sub> cluster compared to the benzene (solvent)<sub>1</sub> cluster which results in an increase of the  $E_a/E_c$  ratio with the increase of cluster size. This strongly favors inhomogeneous nucleation for large benzene(solvent)<sub>n</sub> clusters. Second, as the cluster grows in size the number of bonds over which to distribute the binding energy of the collision partner increases greatly, and thus the ability of the cluster to dissipate the added binding energy increases.

#### VIII. CONCLUSIONS.

Two color time of flight mass spectroscopy has been employed to study small and large clusters of benzene with nitrogen, carbon monoxide, and carbon dioxide created in a supersonic molecular jet. Potential energy calculations, normal coordinate and internal rotational analyses have been employed for the assignment of the  $0_0^0$  and  $6_0^1$  spectra of the benzene(solvent)<sub>1</sub> clusters. Geometries of small clusters ( $n=1,2$ ) have been computer calculated and assigned to experimental spectra. Transition energy shifts for both small and large clusters with up to eight solvent molecules are investigated for the first time as a function of cluster size. The following major conclusions emerge from this study:

1. The calculated cluster binding energies scale well with the solvent polarizabilities: the larger the polarizability the higher the binding energy.
2. The cluster spectral shifts depend on the solute-solvent geometry and interaction but are less dependent on solvent polarizability. The dependence of the energy shift on the cluster geometry is found to be less prominent than in our previous studies of benzene-alkane clusters. Both red and blue

cluster energy shifts are observed and the additive energy shift rule for the isotropic benzene-solvent clusters does not apply in general for the clusters studied.

3. Analysis of the rotational and vibrational motions within the benzene(solvent)<sub>1</sub> clusters makes possible the assignment of the rotational and vdW vibrational modes in the spectra. Both internal rotation modes of the solvent molecule rotating around the solute-solvent bond axis and vdW vibrations are active in the benzene(solvent)<sub>1</sub> cluster spectra and must be accounted for. All three solvent molecules studied rotate nearly freely around the benzene-solvent bond axis. The spectra are well assigned assuming no barrier to rotation in the ground state (free rotor) and a small ca. 20 cm<sup>-1</sup> barrier to rotation in the excited state (slightly hindered rotor). The solvent rotational axis for these linear diatomic and triatomic molecular solvents is oriented along the benzene-solvent bond and thus little or no barrier for the internal rotation exists.

4. The benzene(solvent)<sub>1</sub> vdW vibrations observed are those involving bending motions parallel to the benzene molecular plane ( $b_x$  and  $b_y$ ), a stretching motion along the solute-solvent bond ( $S_z$ ), and a torsional motion ( $t_y$ ). The  $t_z$  motion is not present because of the free rotation around the z axis.

5. Differences pertaining to energy shifts, intensity distribution and appearance of the rotational and vdW modes are found between the  $0_0^0$  and  $6_0^1$  cluster spectra. These differences arise mostly from different selection rules: the origin is allowed at the  $6_0^1$  transition but forbidden at the  $0_0^0$ . Consequently, relatively weak internal rotational mode structure is identified in the  $0_0^0$  spectra but is difficult to distinguish in the  $6_0^1$  spectra which are dominated by a strong origin and associated vdW vibrations.

6. Large vdW clusters of up to eight  $N_2$  molecules and seven  $CO_2$  molecules solvating benzene are observed for the first time. One rather broad cluster feature dominates the spectra. A linear energy shift to the red with increasing cluster size is found. The cluster shifts are not saturated by one solvent molecule on each side of the aromatic ring as was found previously for small benzene-alkane clusters. This may be due to the relatively small size of the solvent molecules.

7. Homogeneous nucleation is found to dominate the formation of small benzene(solvent)<sub>2</sub> clusters. This is due to a very small solvent dimer binding energy with respect to the cluster binding energy. In large clusters the ratio of the solvent aggregate binding energy to the cluster binding energy and the number of ways to share the binding energy between the cluster bonds increase considerably; hence, inhomogeneous nucleation may be favored in the formation of large clusters.

#### ACKNOWLEDGMENTS

One of us (Romuald Nowak) appreciates many helpful discussions concerning molecular symmetry groups with Hoong-Sun Im (Colorado State University). We wish to thank C. Lilly, B. LaRoy, K. Cox and J.I. Seeman (Philip Morris Research Center U.S.A.) for their support and assistance in this research.

## REFERENCES

1. M. Schauer and E.R. Bernstein, *J. Chem. Phys.* **82**, 726 (1985).
2. M. Schauer, K.S. Law and E.R. Bernstein, *J. Chem. Phys.* **82**, 736 (1985).
3. J. Wanna and E.R. Bernstein, *J. Chem. Phys.* **84**, 927 (1986).
4. J. Wanna, J.A. Menapace and E.R. Bernstein, *J. Chem. Phys.* **85**, 1795 (1986).
5. J.A. Menapace and E.R. Bernstein, *J. Phys. Chem.* **91**, 2533 (1987).
6. J.A. Menapace and E.R. Bernstein, *J. Phys. Chem.* **91**, 2843 (1987).
7. K. Okuyama, N. Mikami and I. Ito, *J. Phys. Chem.* **89**, 5617 (1985).
8. P.J. Breen, J.A. Warren and E.R. Bernstein, *J. Chem. Phys.* **87**, 1917 (1987).
9. J. Forges, M.F. Feraudy, B. Raoult and G. Torchet, *J. Chem. Phys.* **78**, 5067 (1983).
10. G. Torchet, H. Bouchier, J. Farges, M.S. de Feraudy and B. Raoult, *J. Chem. Phys.* **81** 2137 (1984).
11. J.A. Barnes and T.E. Gough, *J. Chem. Phys.* **86**, 6012 (1987).
12. E.R. Bernstein, K. Law and M. Schauer, *J. Chem. Phys.* **80**, 207 (1984).
13. E.B. Wilson Jr., J.C. Decius and P.C. Cross, "Molecular Vibrations, Theory of Infrared and Raman Vibrational Spectra" (McGraw-Hill, New York, 1955).
14. G. Herzberg, "Molecular Spectra and Molecular Structure: II. Infrared and Raman Spectra of Polyatomic Molecules" (Van Nostrand-Reinhold, New York, 1945).
15. P. Bunker, "Molecular Symmetry and Spectroscopy" (Academic Press, London, 1979).
16. C.J. Bradley and A.P. Cracknell, "The Mathematical Theory of Symmetry in Solids" (Clarendon Press, Oxford, 1972).
17. S. Li, R. Nowak and E.R. Bernstein, unpublished results.
18. R. Nowak and E.R. Bernstein, *J. Chem. Phys.* **86**, 4783 (1987).

TABLE I

Rovibronic and nuclear spin selection rules.

+ and - stand for an allowed and forbidden transition, respectively.

Transitions not indicated are completely forbidden.

Cluster	Molecular Symmetry Group	Possible Transitions	Selection Rules	
			Rovibronic $0_0^0 \rightarrow 6_0^1$	Nuclear Spin
benzene(N <sub>2</sub> ) <sub>1</sub> & benzene(CO <sub>2</sub> ) <sub>2</sub>	G <sub>24</sub> <sup>5</sup>	a <sub>1g</sub> ↔ a <sub>1g</sub>	-	+
		e <sub>2g</sub> ↔ e <sub>2g</sub>	+	+
		a <sub>1g</sub> ↔ e <sub>2g</sub>	+	+
		e <sub>1u</sub> ↔ e <sub>1u</sub>	+	+
		b <sub>2u</sub> ↔ b <sub>2u</sub>	-	+
		e <sub>1u</sub> ↔ b <sub>2u</sub>	+	+
benzene(CO) <sub>1</sub>	G <sub>12</sub> <sup>3</sup>	a <sub>1</sub> ↔ a <sub>1</sub>	-	+
		e <sub>2</sub> ↔ e <sub>2</sub>	+	+
		a <sub>1</sub> ↔ e <sub>2</sub>	+	+
		e <sub>1</sub> ↔ e <sub>1</sub>	+	+
		b <sub>2</sub> ↔ b <sub>2</sub>	-	+
		e <sub>1</sub> ↔ b <sub>2</sub>	+	+

TABLE II

Assignments of the  $0_0^0$  and  $6_0^1$  benzene(N<sub>2</sub>)<sub>1</sub> cluster spectra.

Transition Region	Experimental Peak Positions (Relative to cluster origin)  cm <sup>-1</sup>	Calculated Rotational Transitions		Calculated vdW Vibrations	
		Value cm <sup>-1</sup>	Assignment	Value cm <sup>-1</sup>	Assignment
$0_0^0$ (Fig. 3a) [38,122 cm <sup>-1</sup> ]	-23	-24	$4e_{2g} \leftarrow 2e_{2g}$	-	
	-8	-8	$2e_{2g} \leftarrow 0a_{1g}$	-	
	-6	-1	$2e_{2g} \leftarrow 2e_{2g}$	-	
	-1	1	$4e_{2g} \leftarrow 4e_{2g}$	-	
	9	7	$0a_{1g} \leftarrow 2e_{2g}$	-	
	23	25	$2e_{2g} \leftarrow 4e_{2g}$	23	$b_x^2$
	37	32	$0a_{1g} \leftarrow 4e_{2g}$	31	$b_y^2$
	50	-	-	46	$b_x^4$
$6_0^1$ (Fig. 3b) [38,602 cm <sup>-1</sup> ]	65	-	-	62:60	$b_y^4; s_z$
	32	25	$2e_{2g} \leftarrow 4e_{2g}$	23	$b_x^2$
	37	32	$0a_{1g} \leftarrow 4e_{2g}$	31	$b_y^2$
	41			46	$b_x^4$
	67			61:60	$b_y^4; s_z$
	106			102	$t_y^2$

TABLE III

Assignments of the  $0_0^0$  and  $6_0^1$  benzene(CO<sub>2</sub>)<sub>1</sub>  
cluster spectra shown in Fig. 4.

Transition Region	Experimental Peak Positions (Relative to cluster origin)  cm <sup>-1</sup>	Calculated Rotational Transitions		Calculated vdW Vibrations	
		Value cm <sup>-1</sup>	Assignment	Value cm <sup>-1</sup>	Assignment
$0_0^0$ (Fig. 4a) [38,085 cm <sup>-1</sup> ]	-6	-7	$2e_{2g} \leftarrow 0a_{1g}$	-	
	-1	-1	$2e_{2g} \leftarrow 2e_{2g}$	-	
	1	1	$4e_{2g} \leftarrow 4e_{2g}$	-	
	7	6	$0a_{1g} \leftarrow 2e_{2g}$	-	
	17	19	$2e_{2g} \leftarrow 4e_{2g}$	-	
	25	26	$0a_{1g} \leftarrow 4e_{2g}$	-	
	33	-		35;38	$b_x^2; b_y^2$
	65	-		72;70	$s_z; b_x^4$
$6_0^1$ (Fig. 4b) [38,612 cm <sup>-1</sup> ]	9	6	$0a_{1g} \leftarrow 2e_{2g}$	-	
	16	19	$2e_{2g} \leftarrow 4e_{2g}$	-	
	28	26	$0a_{1g} \leftarrow 4e_{2g}$	-	
	51	-		35	$b_x^2$
	54	-		38	$b_y^2$
	63	-		71;70	$s_z; b_x^4$
	70	-		70;76	$b_x^4; b_y^4$

**TABLE IV**

Assignments of the  $0_0^0$  and  $6_0^1$  benzene(CO)<sub>1</sub>  
cluster spectra shown in Fig. 6.

Transition Region	Experimental Peak Positions (Relative to cluster origin)  cm <sup>-1</sup>	Calculated Rotational Transitions		Calculated vdW Vibrations	
		Value cm <sup>-1</sup>	Assignment	Value cm <sup>-1</sup>	Assignment
$0_0^0$ (Fig. 6a)  [38,110 cm <sup>-1</sup>	-23	-24	$4e_2 \leftarrow 2e_2$	-	
	-15	-16	$3b_2 \leftarrow 0a_1$	-	
	-8	-8	$2e_2 \leftarrow 0a_1$	-	
	0	-1	$2e_2 \leftarrow 2e_2$	-	
	0	0.5	$3b_2 \leftarrow 3b_2$	-	
	0	1	$4e_2 \leftarrow 4e_2$	-	
	10	7	$0a_1 \leftarrow 2e_2$		
	10	11	$0a_1 \leftarrow 3b_2$	14	$b_x$
	23	21	$0a_1 \leftarrow 3b_2$	18	$b_y$
	23	24.5	$2e_2 \leftarrow 4e_2$		
	35	33	$0a_1 \leftarrow 4e_2$		
	42	-	-	42	$b_x^3$
	55			54	$t_y, b_y^3$
	66			68	$s_z$



TABLE IV - Continued...2 of 2.

Transition Region	Experimental Peak Positions (Relative to cluster origin)  cm <sup>-1</sup>	Calculated Rotational Transitions		Calculated vdW Vibrations	
		Value cm <sup>-1</sup>	Assignment	Value cm <sup>-1</sup>	Assignment
6 <sub>0</sub> <sup>1</sup>  (Fig. 6b)  [38,592 cm <sup>-1</sup> ]	7	7	0a <sub>1</sub> ← 2e <sub>2</sub>	-	-
	11	11	0a <sub>1</sub> ← 3b <sub>2</sub>	-	-
	-	21	0a <sub>1</sub> ← 3b <sub>2</sub>	-	-
	-	21.6	2e <sub>2</sub> ← 4e <sub>2</sub>	-	-
	33	33	0a <sub>1</sub> ← 4e <sub>2</sub>	28	b <sub>x</sub> <sup>2</sup>
	38	-	-	36	b <sub>y</sub> <sup>2</sup>
	46	-	-	42	b <sub>x</sub> <sup>3</sup>
	-	-	-	54	t <sub>y</sub> , b <sub>y</sub> <sup>3</sup>
	69	-	-	68	s <sub>z</sub>
	76	-	-	72	b <sub>y</sub> <sup>4</sup>

TABLE V

Calculated binding energies for various clusters and solvent aggregates,  
relative intensities of peaks due to isotropic versus anisotropic  
clusters ( $I_{\text{iso}}/I_{\text{aniso}}$ ) and solvent molecular polarizabilities.

solvent	$E_d$ solvent dimer binding energy <sup>a)</sup> cm <sup>-1</sup>	$E_t$ solvent trimer binding energy <sup>a)</sup> cm <sup>-1</sup>	benzene (solvent) <sub>1</sub> binding energy <sup>a)</sup> cm <sup>-1</sup>	$E_c$ benzene (solvent) <sub>2</sub> binding energy <sup>a)</sup> cm <sup>-1</sup>	$E_d/E_c$ (anisotropic cluster)	$I_{\text{iso}}/I_{\text{aniso}}$ b)	Solvent Polariz ability $10^{25} \text{ cm}^3$
				isotropic cluster	anisotropic cluster		
N <sub>2</sub>	-150	-440	-501	-1007	-962	-2-7	17.6
CO	-452	-1114	-612	-1283	-1626 <sup>d)</sup>	-	19.5
CO <sub>2</sub>	442	1312	-868	-1746	-1955	-1.5-2	26.5

a) obtained from the minimum potential energy calculations.

b) this value depends on the ionization energy (see also Fig. 8).

c) J.O. Hirschfelder, C.F. Curtiss and R.B. Bird, Molecular Theory of Gases and Liquids, (John Wiley, 1964).

d) average energy of three calculated conformers.

### FIGURE CAPTIONS

- Figure 1** Calculated ground state minimum energy configuration (a) and eigenvalues and eigenvectors of the vdW modes (b-f) for benzene(N<sub>2</sub>)<sub>1</sub>. Rigid cluster symmetry is taken to be C<sub>2v</sub>.
- Figure 2** Energies of the internal rotational levels of the N<sub>2</sub> molecule in the benzene(N<sub>2</sub>)<sub>1</sub> cluster calculated with  $B = 1.917 \text{ cm}^{-1}$  as a function of a  $V_6$  potential barrier. The symmetries of the free rotor rotational levels at  $0 \text{ cm}^{-1}$ , in order of increasing energy, are  $0a_{1g}$ ,  $1e_{1u}$ ,  $2e_{2g}$ ,  $3b_{2u}$ ,  $4e_{2g}$ ,  $5e_{1u}$ ,  $6a_{1g}$  and  $7e_{1u}$ .
- Figure 3** Two color TOFMS of the benzene(N<sub>2</sub>)<sub>1</sub> cluster in the  $0_0^0$  (a) and  $6_0^1$  (b) regions. The internal rotational (continuous line) and vdW vibrational (dashed line) transitions are calculated as described in the text with the potential barrier in the excited state  $V_6 (S_1) = 20 \text{ cm}^{-1}$ . The 0 energy in the  $0_0^0$  spectrum corresponds to the calculated position of the forbidden origin. The intensities in the calculated spectra are chosen arbitrarily in agreement with the experimental spectra. Specific assignments are given in Table II. The arrows indicate positions of the  $0_0^0$  ( $38086.1 \text{ cm}^{-1}$ ) and  $6_0^1$  ( $38608.5 \text{ cm}^{-1}$ ) transitions in bare benzene.

**Figure 4** Two color TOFMS of the benzene(CO<sub>2</sub>)<sub>1</sub> cluster in the 0<sub>0</sub><sup>0</sup> (a) and 6<sub>0</sub><sup>1</sup> (b) regions. Calculated spectra ( $V_6$  (S<sub>1</sub>) = 16 cm<sup>-1</sup>) consist of rotational (continuous line) and vdW vibrational (dashed line) transitions. The 0 energy corresponds to the calculated position of the forbidden origin. Specific assignments are given in Table III. The arrows indicate corresponding benzene transitions (see caption for Fig. 3). The dip to the left of the origin in b is due to the saturation of the mass detector by ionized benzene molecules.

**Figure 5** Calculated ground state minimum energy configuration for the benzene(CO)<sub>1</sub> cluster. The rigid cluster symmetry is C<sub>s</sub>. The vdW vibrations are very similar to those shown in Fig. 1 for the benzene(N<sub>2</sub>)<sub>1</sub> cluster with the selection rules given in section III.A. The solid line indicates the CO rotational axis.

**Figure 6** Two color TOFMS of the benzene(CO)<sub>1</sub> cluster in the 0<sub>0</sub><sup>0</sup> (a) and 6<sub>0</sub><sup>1</sup> (b) regions. Specific assignments of both experimental and calculated spectra are shown in Table IV. The arrow indicates the benzene origin (compare Fig. 3).

**Figure 7** Calculated ground state minimum energy configurations of benzene(N<sub>2</sub>)<sub>2</sub> clusters: isotropic (a) and anisotropic (b).

**Figure 8** Two color TOFMS of benzene(N<sub>2</sub>)<sub>2</sub> clusters taken at two different ionization energies: 37270 cm<sup>-1</sup> (upper) and 36550 cm<sup>-1</sup> (lower). 0 corresponds to the 6<sub>0</sub><sup>1</sup> transition of benzene at 38608.5 cm<sup>-1</sup>. The most intense peak in the spectrum is assigned to the isotropic cluster

**Figure 9** The benzene(CO<sub>2</sub>)<sub>2</sub> two color TOFMS at 0<sub>0</sub><sup>0</sup> (a) and 6<sub>0</sub><sup>1</sup> (b) transitions. The scale is relative to the benzene transitions.

**Figure 10** Two color TOFMS of the benzene(CO)<sub>2</sub> cluster at 6<sub>0</sub><sup>1</sup>. The scale is relative to benzene 6<sub>0</sub><sup>1</sup> transition.

**Figure 11** Two color TOFMS of the benzene(CO<sub>2</sub>)<sub>3</sub> cluster in the 0<sub>0</sub><sup>0</sup> region.

**Figure 12** The 6<sub>0</sub><sup>1</sup> two color TOFMS of the benzene(N<sub>2</sub>)<sub>n</sub> clusters. The spectra are numbered according to the number of N<sub>2</sub> molecules in the cluster. 0 corresponds to the benzene 6<sub>0</sub><sup>1</sup> transition at 38608.5 cm<sup>-1</sup>.

**Figure 13** The 6<sub>0</sub><sup>1</sup> two color TOFMS of the benzene(CO<sub>2</sub>)<sub>n</sub> clusters. The numbers reflect the number of CO<sub>2</sub> molecules in the cluster. The scale is analogous to that of Fig. 12.

**Figure 14** Clusters transition energy shifts plotted as a function of the cluster size. The error bars indicate uncertainty due to the broadness of the spectral features.

Benzene(N<sub>2</sub>)<sub>1</sub>

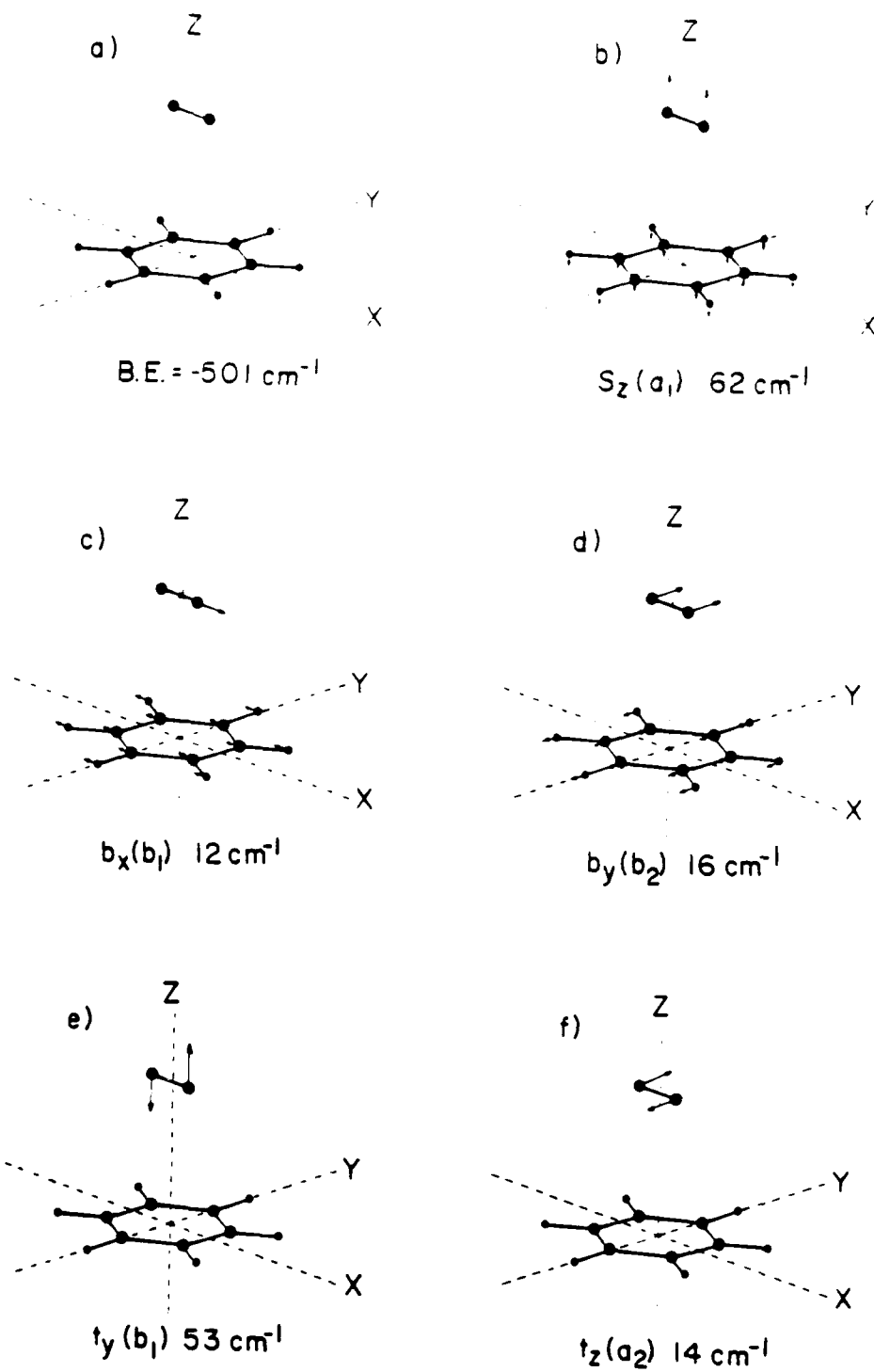


Fig. 1

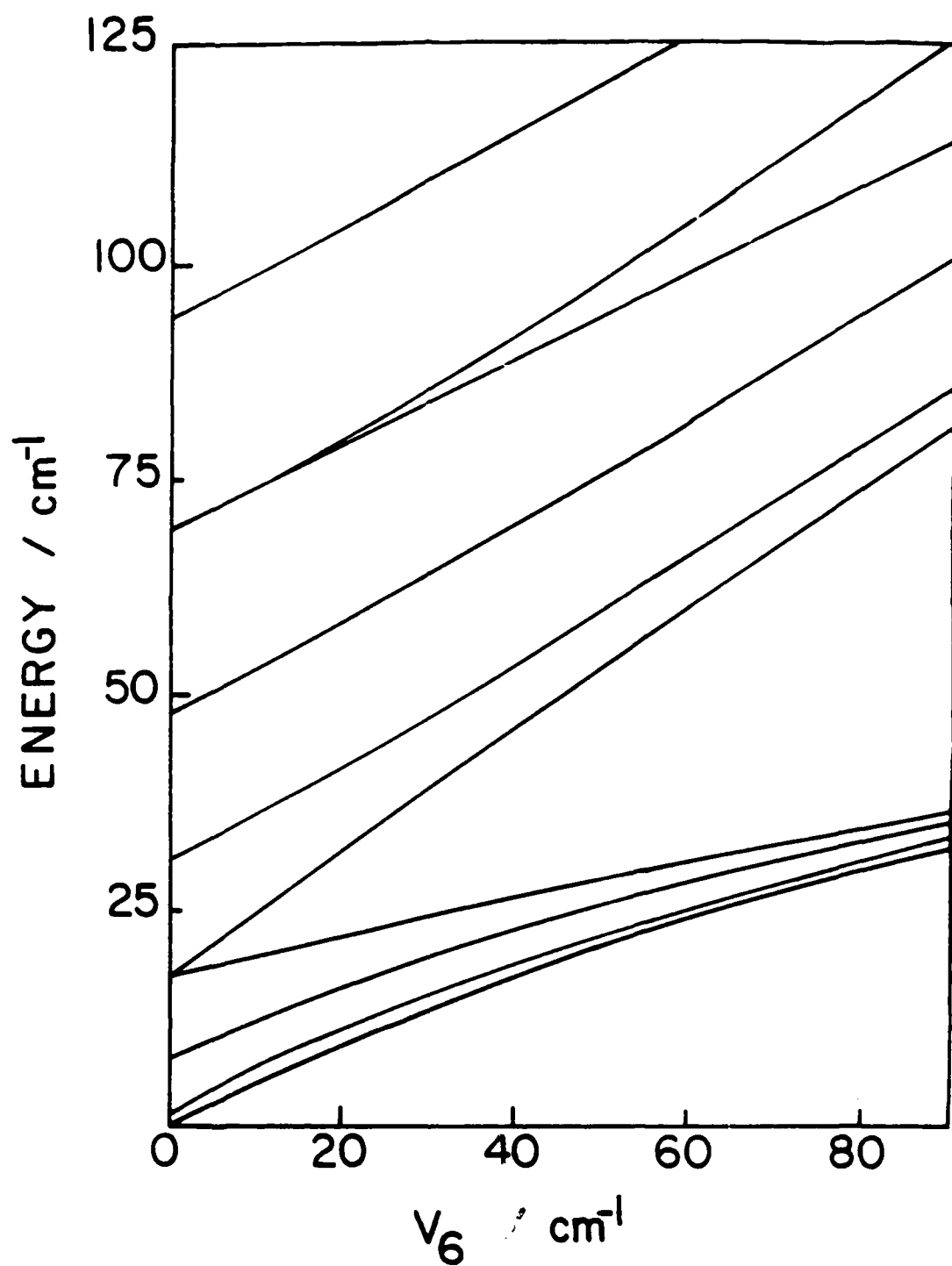


Fig. 2

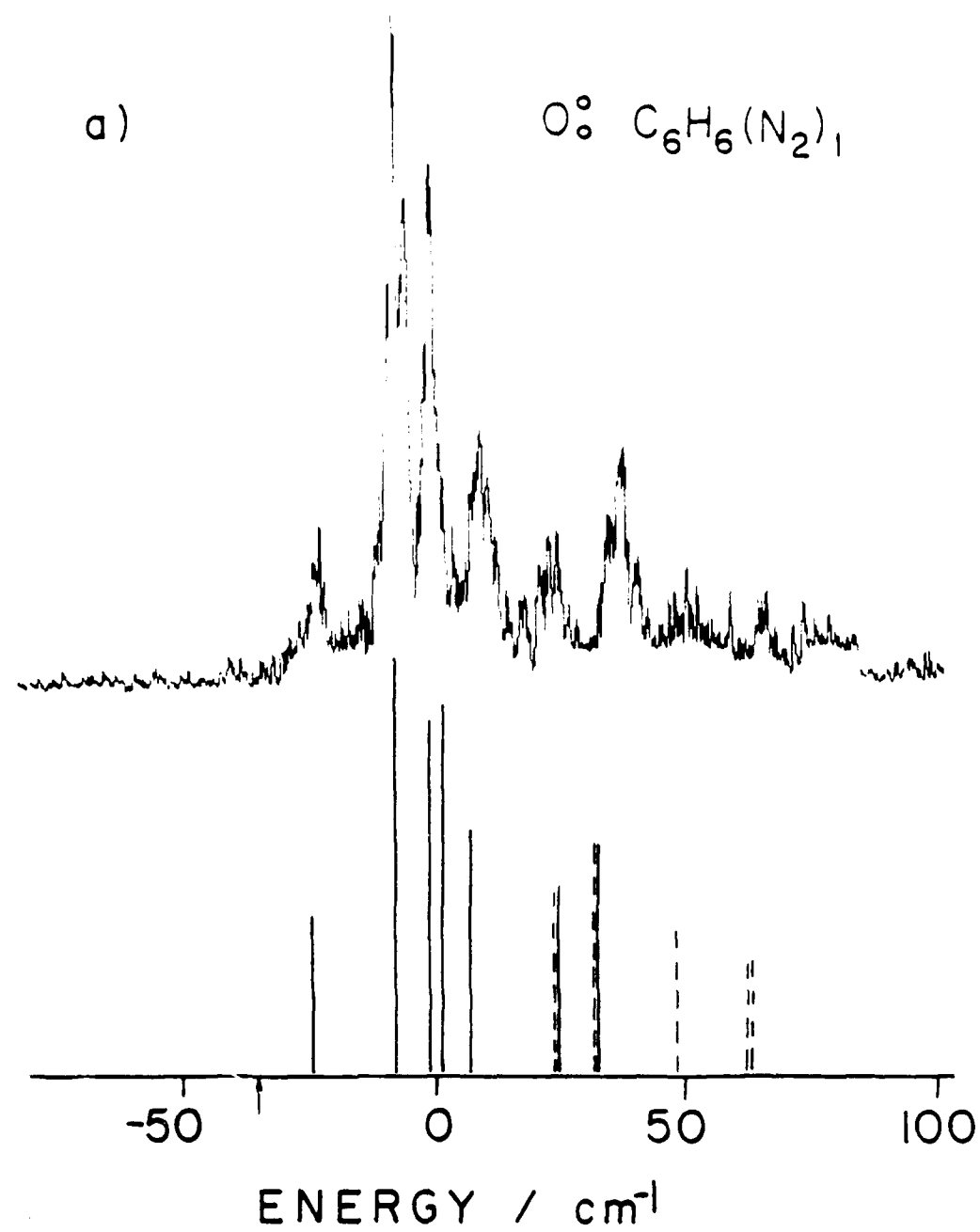


Fig. 3a



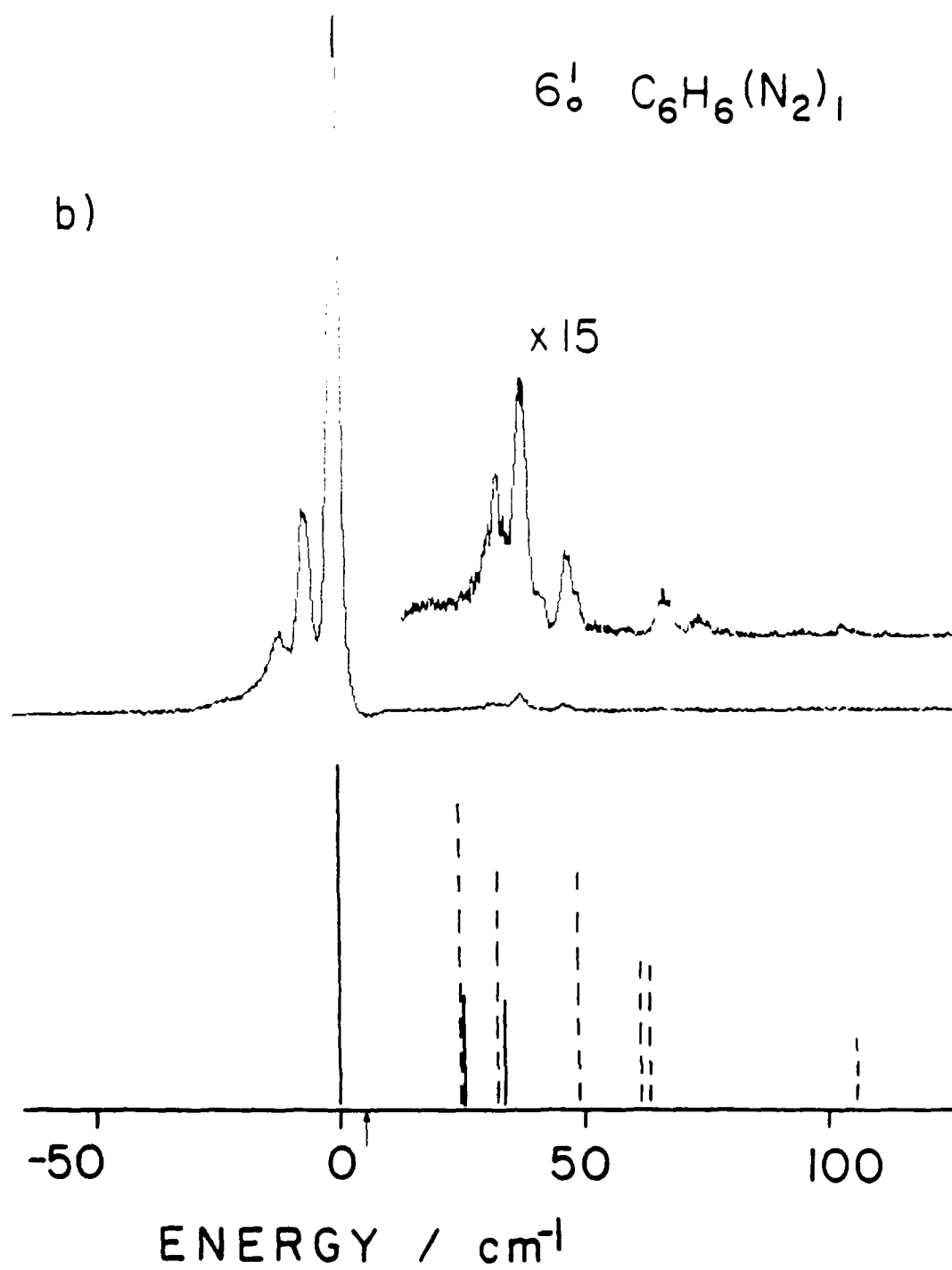


Fig. 3b

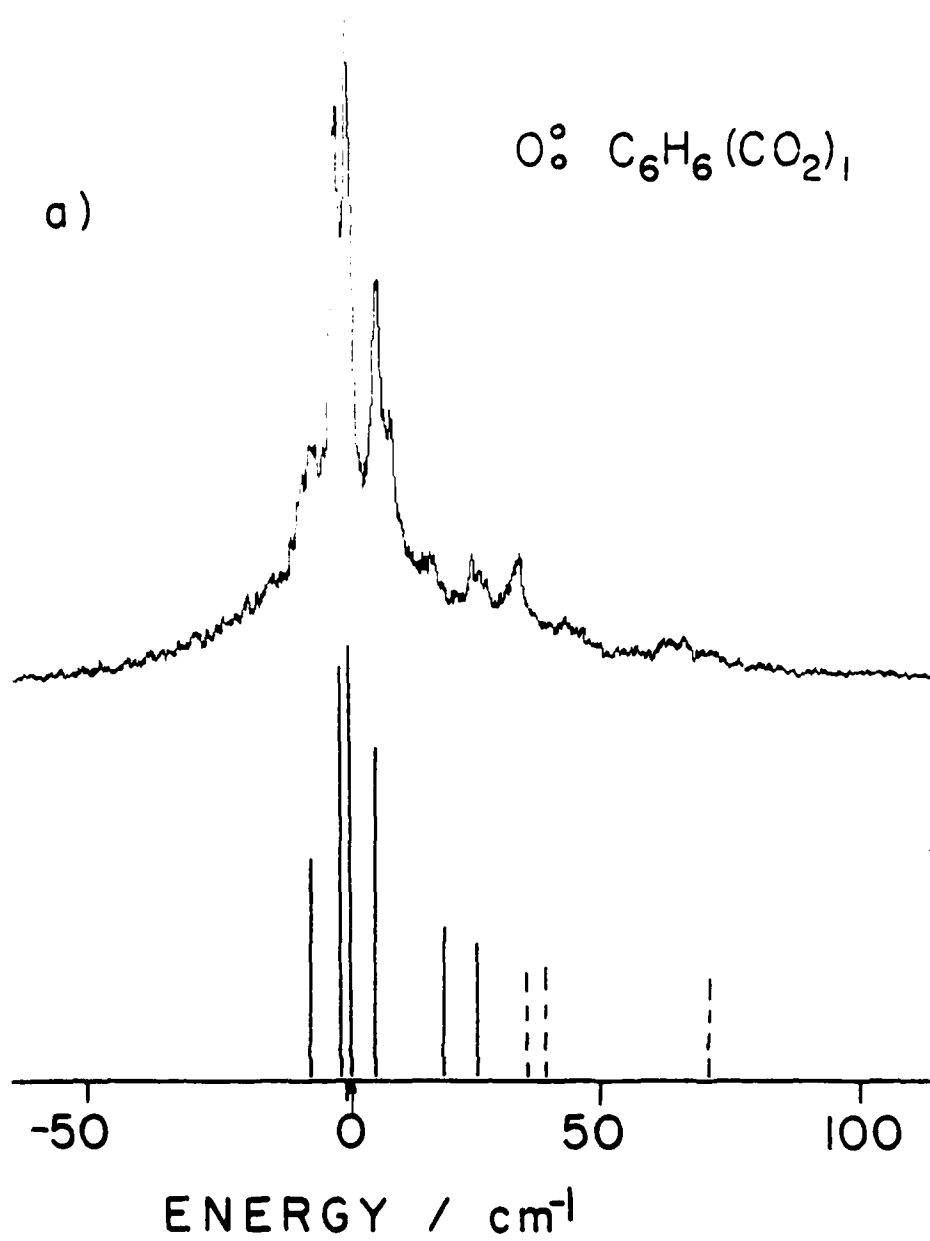


Fig. 4a

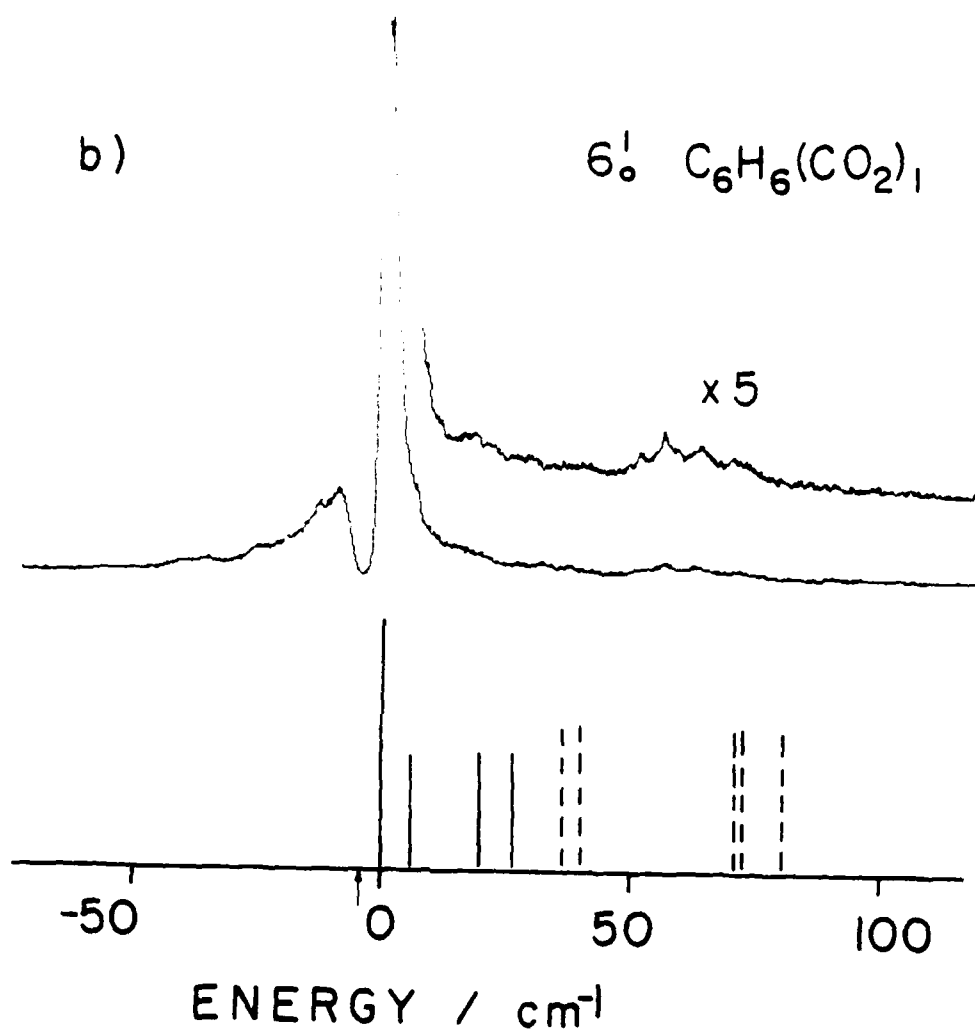


Fig. 4b

Benzene (CO)<sub>1</sub>

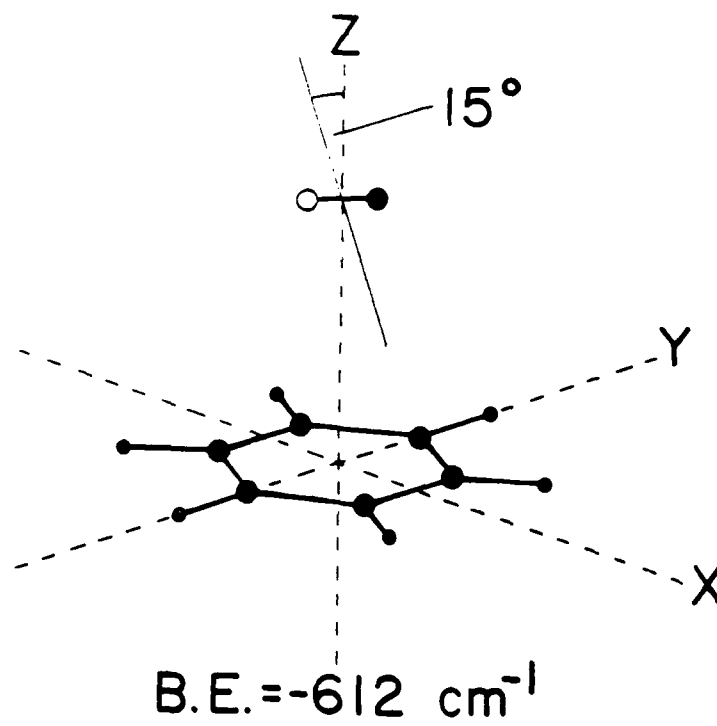


Fig. 5

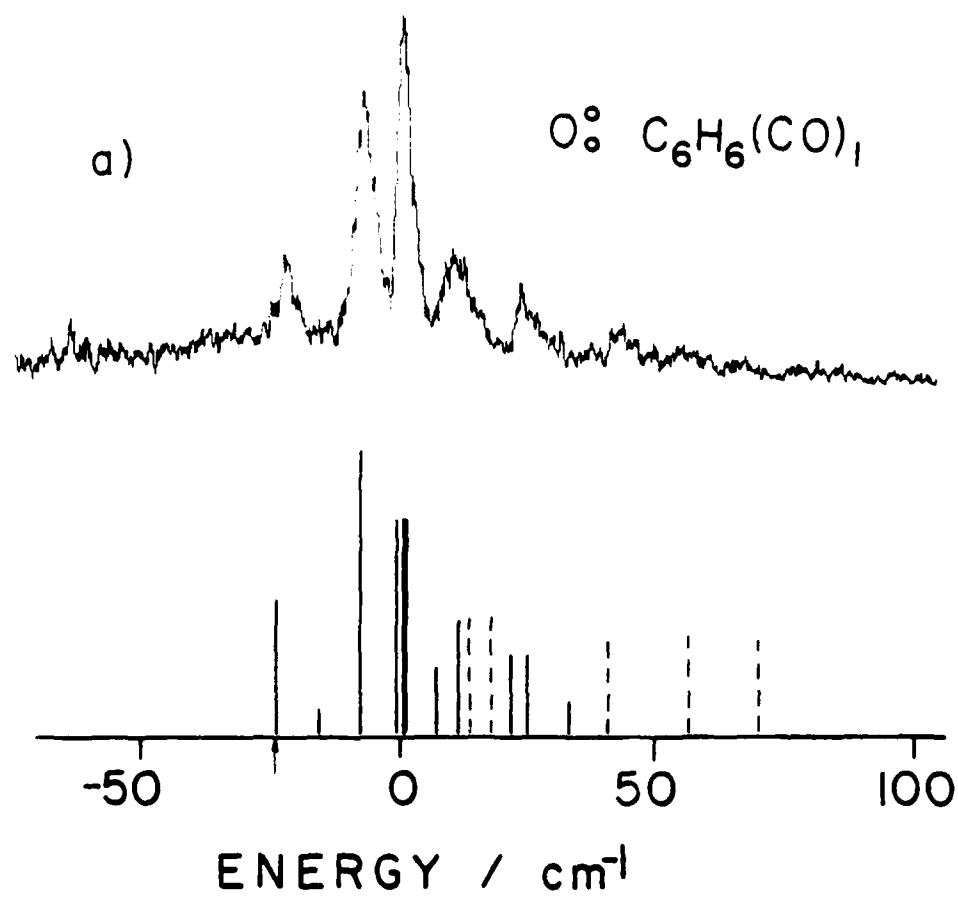


Fig. 6a

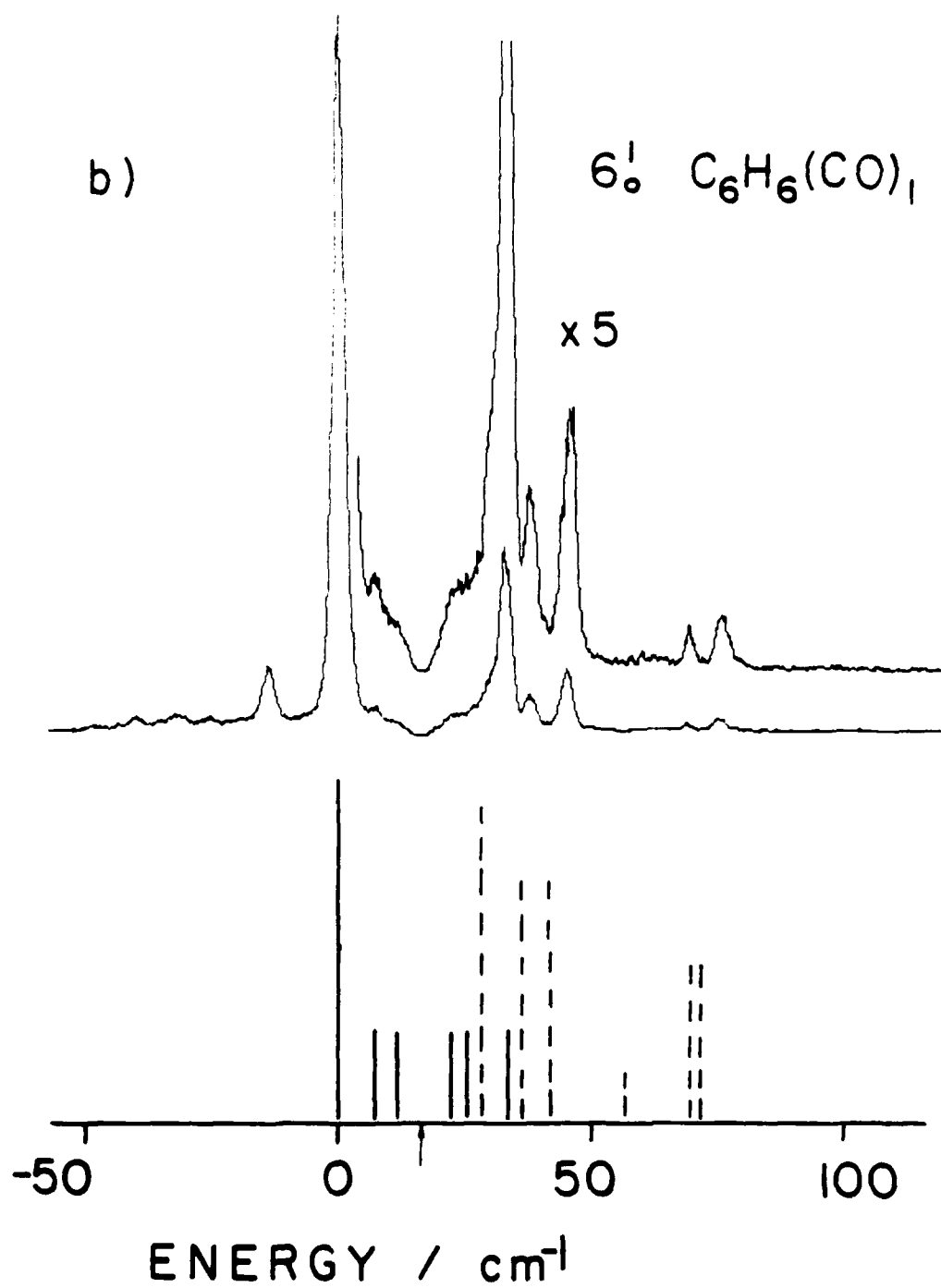


Fig. 6b

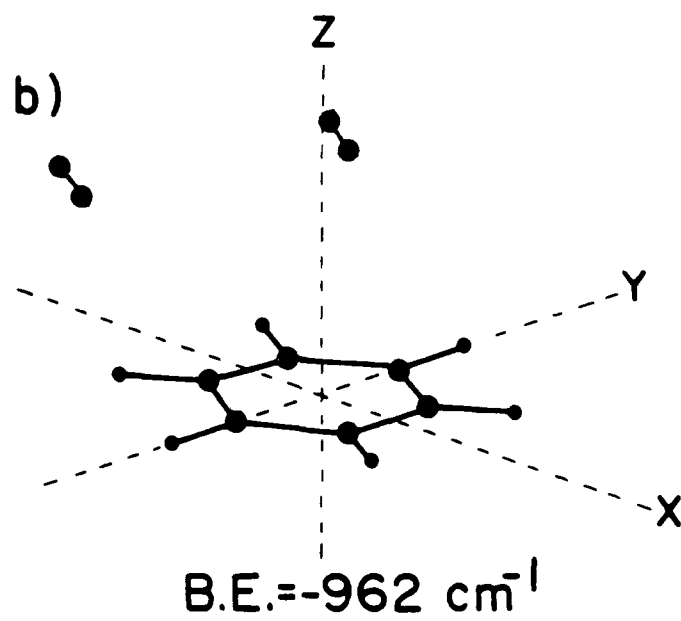
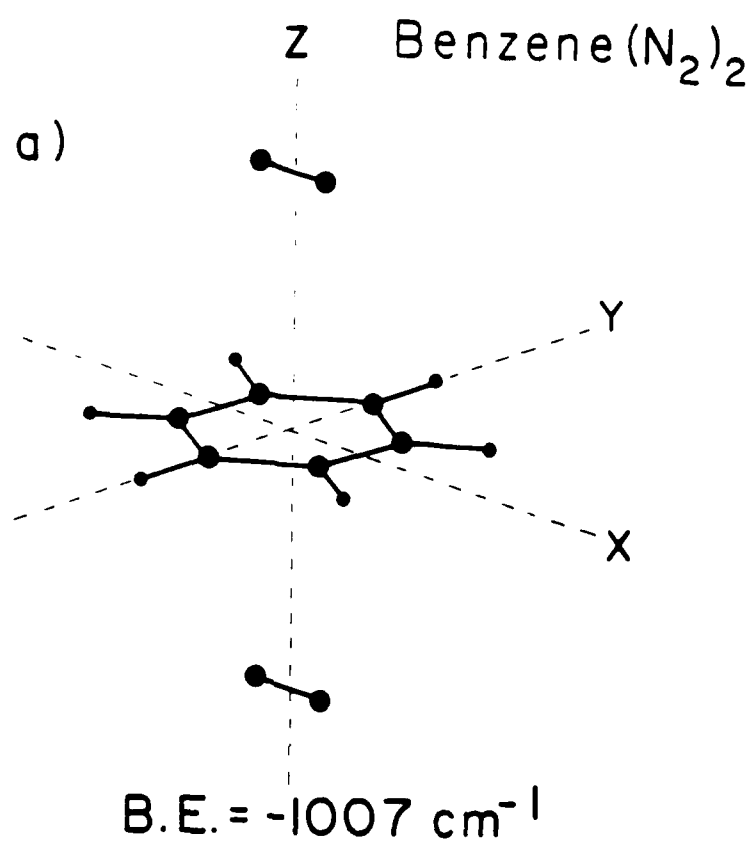


Fig. 7

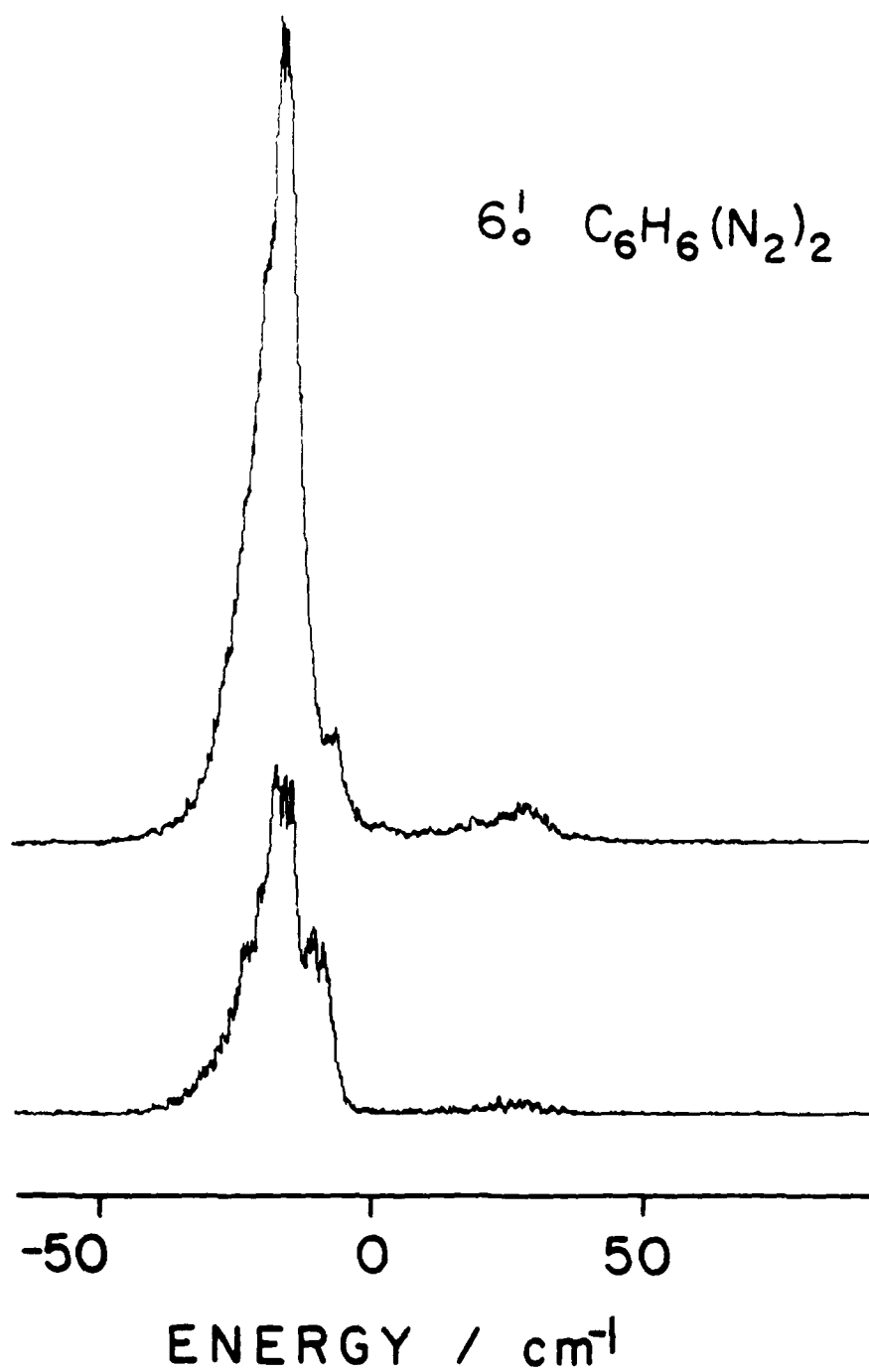


Fig. 3



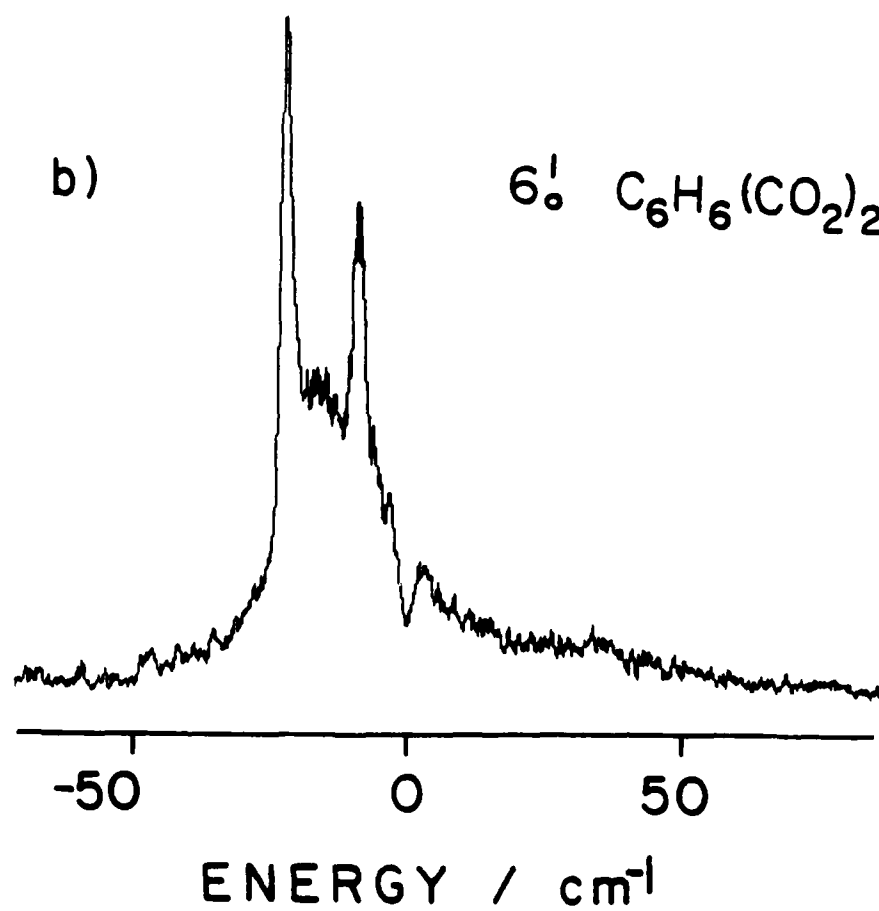
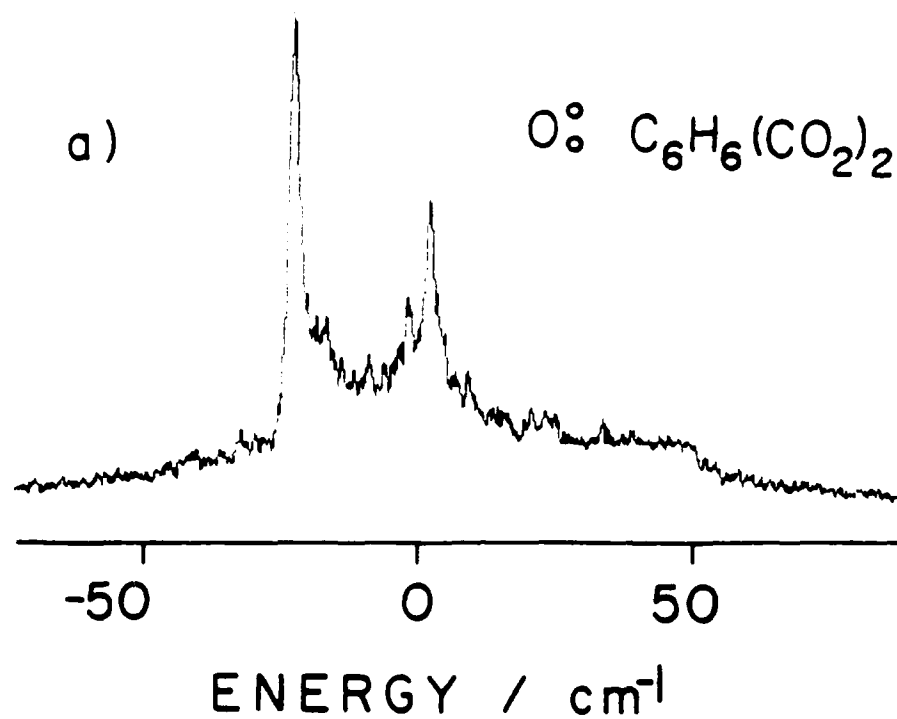


Fig. 9

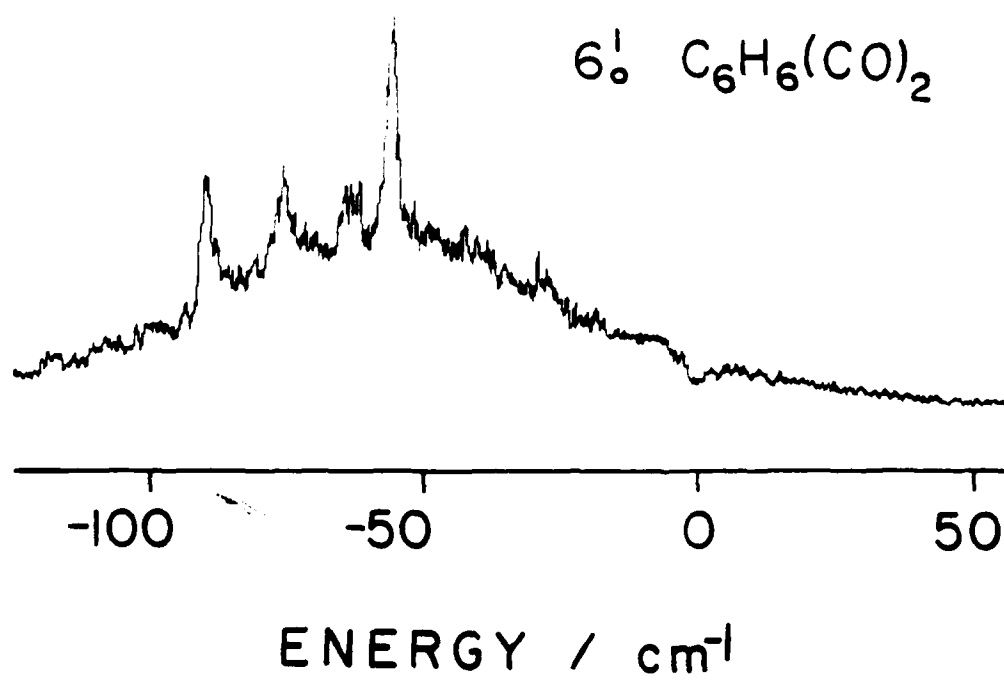


Fig. 10

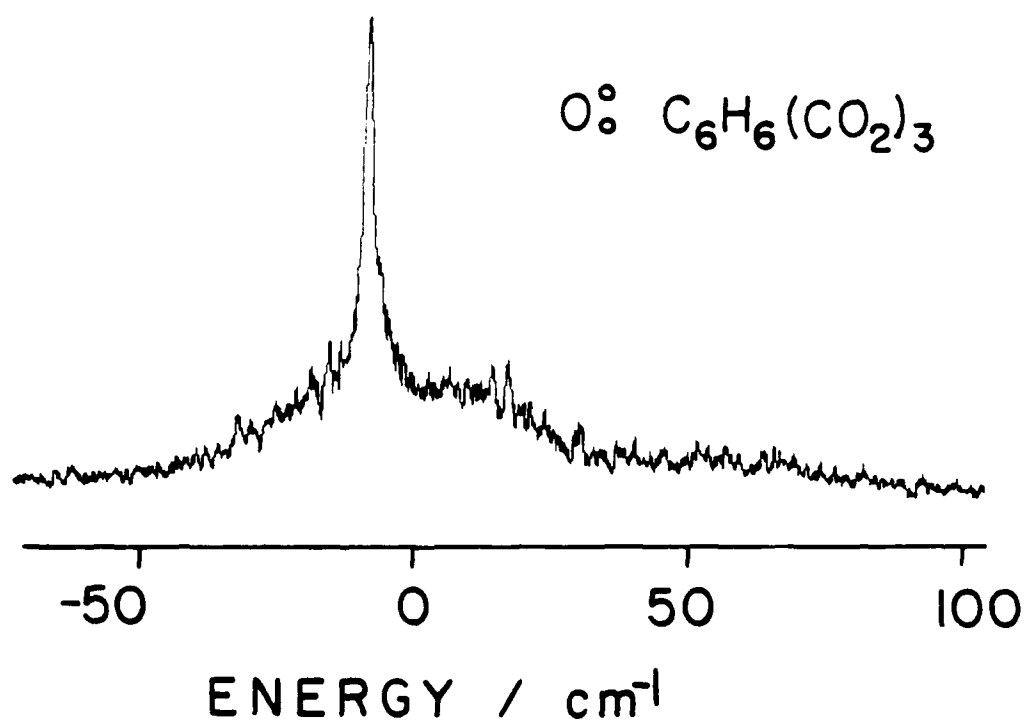


Fig. 11

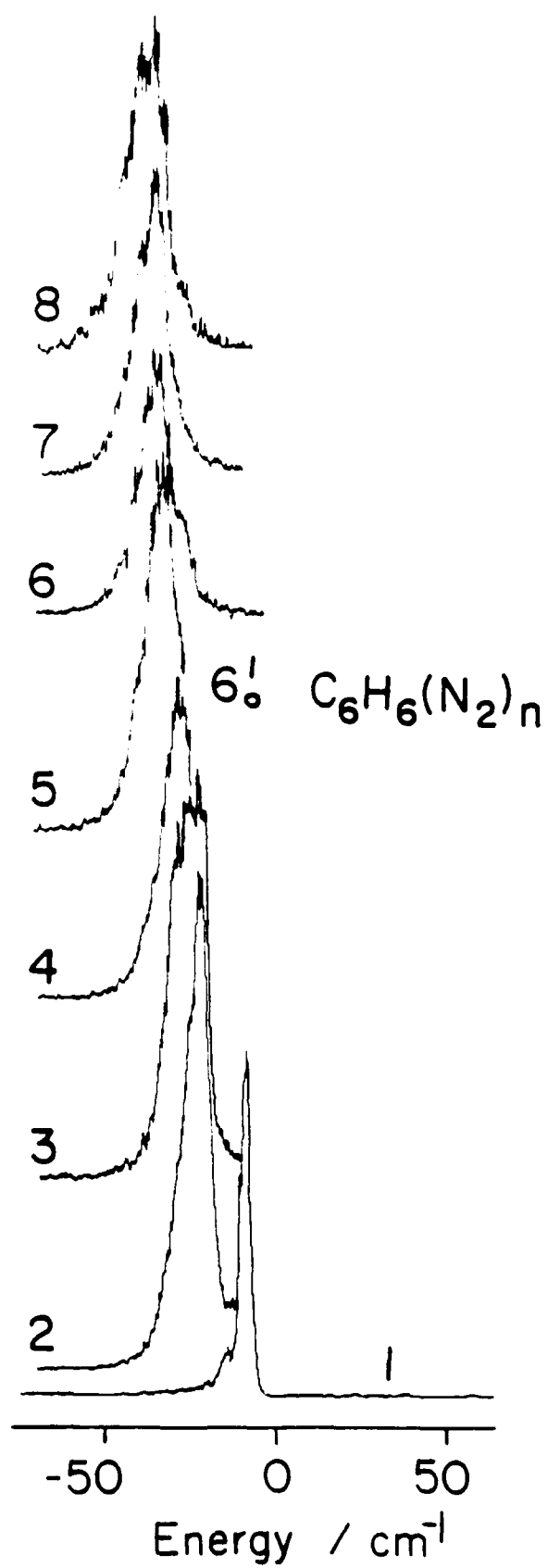


Fig. 12

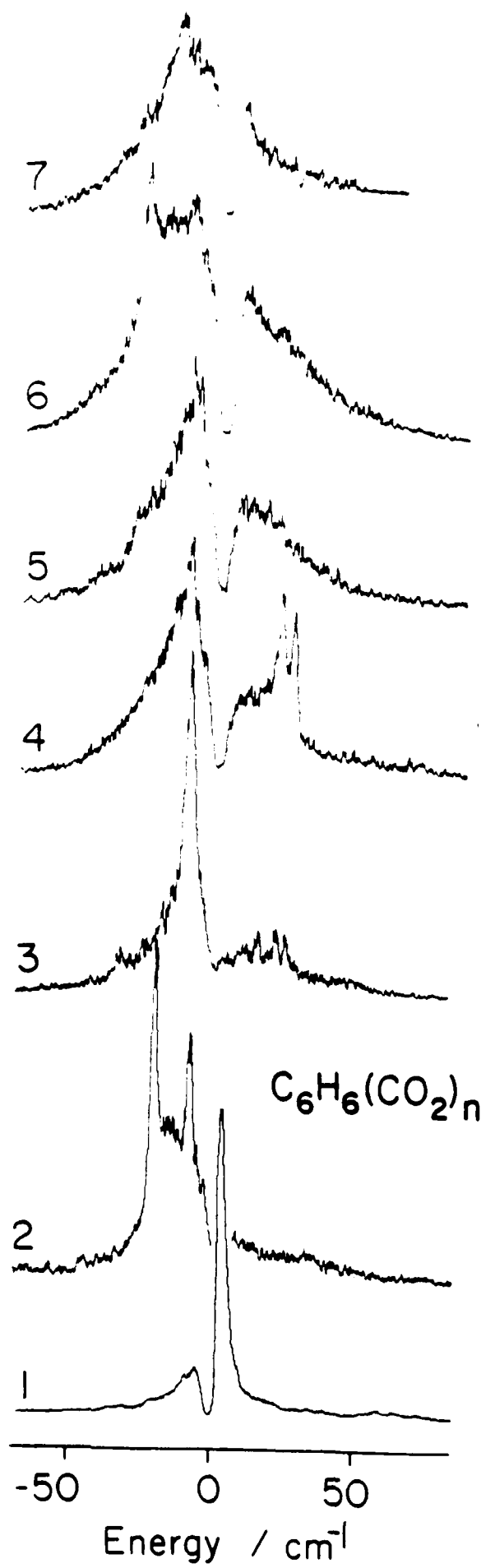


Fig. 13

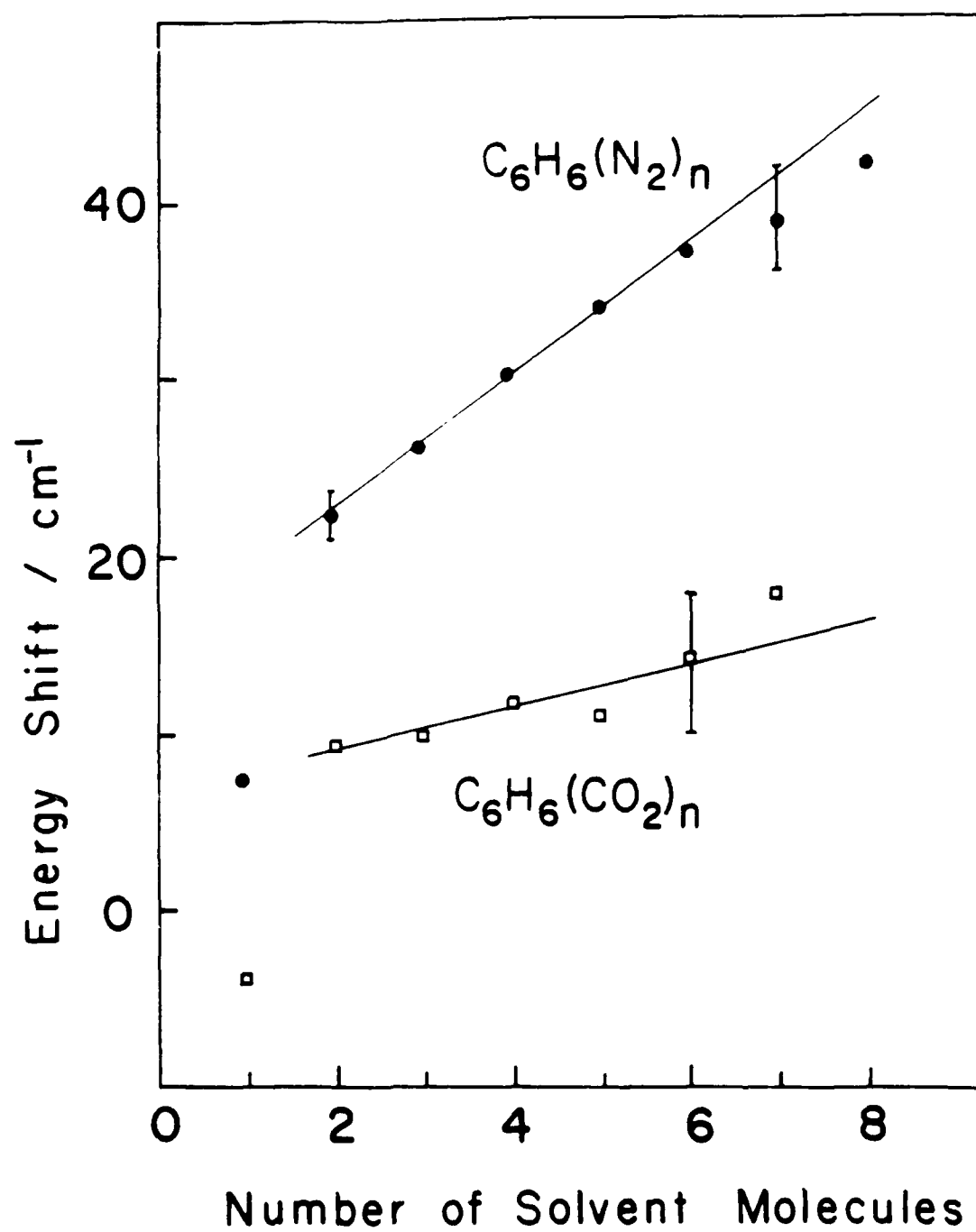


Fig. 14

TECHNICAL REPORT DISTRIBUTION LIST, GEN

	<u>No.</u> <u>Copies</u>		<u>No.</u> <u>Copies</u>
Office of Naval Research ATTN: Code 413 800 North Quincy Street Arlington, VA 22217	2	Dr. David Young Code 334 NORDA NSTL, MS 39529	1
Dr. Bernard Doua Naval Weapons Support Center Code 5042 Crane, IN 47522	1	Naval Weapons Center ATTN: Dr. A. B. Amster Chemistry Division China Lake, CA 93555	1
Commander, Naval Air Systems Command ATTN: Code 310C (H. Rosenwasser) Washington, DC 20360	1	Scientific Advisor Commandant of the Marine Corps Code RD-1 Washington, DC 20380	1
Naval Civil Engineering Laboratory ATTN: Dr. R. W. Drisko Port Hueneme, CA 93401	1	U.S. Army Research Office ATTN: CRD-AA-IP P.O. Box 12211 Research Triangle Park, NC 27709	1
Defense Technical Information Center Building 5, Cameron Station Alexandria, VA 22314	12	Mr. John Boyle Materials Branch Naval Ship Engineering Center Philadelphia, PA 19112	
DTNSRDC ATTN: Dr. G. Bosmajian Applied Chemistry Division Annapolis, MD 21401	1	Naval Ocean Systems Center ATTN: Dr. S. Yamamoto Marine Sciences Division San Diego, CA 91232	
Dr. William Tolles Superintendent Chemistry Division, Code 6100 Naval Research Laboratory Washington, DC 20375	1		

TECHNICAL REPORT DISTRIBUTION LIST, 051A

Dr. M. A. El-Sayed  
Department of Chemistry  
University of California  
Los Angeles, CA 90024

Dr. E. R. Bernstein  
Department of Chemistry  
Colorado State University  
Fort Collins, CO 80523

Dr. J. R. McDonald  
Chemistry Division  
Naval Research Laboratory  
Code 6110  
Washington, DC 20375-5000

Dr. G. B. Schuster  
Chemistry Department  
University of Illinois  
Urbana, IL 61801

Dr. J. B. Halpern  
Department of Chemistry  
Howard University  
Washington, DC 20059

Dr. M. S. Wrighton  
Department of Chemistry  
Massachusetts Institute of Technology  
Cambridge, MA 02139

Dr. A. Paul Schaap  
Department of Chemistry  
Wayne State University  
Detroit, MI 49207

Dr. W. E. Moerner  
I.B.M. Corporation  
Almaden Research Center  
650 Harry Road  
San Jose, CA 95120-6099

Dr. A. B. P. Lever  
Department of Chemistry  
York University  
Downsview, Ontario  
CANADA M3J 1P3

Dr. John Cooper  
Code 6173  
Naval Research Laboratory  
Washington, DC 20375-5000

Dr. George E. Walrafen  
Department of Chemistry  
Howard University  
Washington, DC 20059

Dr. Joe Brandelik  
AFWAL/AADO-1  
Wright Patterson AFB  
Fairborn, OH 45433

Dr. Carmen Ortiz  
Consejo Superior de  
Investigaciones Cientificas  
Serrano 121  
Madrid 6  
SPAIN

Dr. John J. Wright  
Physics Department  
University of New Hampshire  
Durham, NH 03824

Dr. Kent R. Wilson  
Chemistry Department  
University of California  
La Jolla, CA 92093

Dr. G. A. Crosby  
Chemistry Department  
Washington State University  
Pullman, WA 99164

Dr. Theodore Pavlopoulos  
NOSC  
Code 521  
San Diego, CA 91232